The Impact of Short-Lived Pollutants on Arctic Climate

P.K. Quinn, T.S. Bates, E. Baum, T. Bond, J.F. Burkhart, A.M. Fiore, M. Flanner, T.J. Garrett, D. Koch, J. McConnell, D. Shindell, and A. Stohl

AMAP

Arctic Monitoring and Assessment Programme

Authors: P.K. Quinn[1], T.S. Bates[1], E. Baum[2], T. Bond[3], J.F. Burkhart[4], A.M. Fiore[5], M. Flanner[6], T.J. Garrett[7], D. Koch[8], J. McConnell[9], D. Shindell[8], and A. Stohl[4]

[1] NOAA Pacific Marine Environmental Laboratory, Seattle, WA, USA
[2] Clean Air Task Force, Boston, MA, USA
[3] University of Illinois
[4] Norwegian Institute for Air Research, Kjeller, Norway
[5] NOAA Geophysical Fluid Dynamics Laboratory, Princeton, NJ, USA
[6] Advanced Study Program, NCAR, Boulder, CO, USA
[7] University of Utah, Salt Lake City, UT, USA
[8] NASA Goddard Institute for Space Sciences, New York, NY, USA
[9] Desert Research Institute

1. Introduction

Arctic temperatures have increased at almost twice the global average rate over the past 100 years (IPCC, 2007). From 1954 to 2003, annual average surface air temperatures have increased from 2 to 3°C in Alaska and Siberia and up to 4°C during the winter months (ACIA, 2004). Warming in the Arctic has been accompanied by an earlier onset of spring melt, a lengthening of the melt season, and changes in the mass balance of the Greenland ice sheet (Stroeve et al., 2006; Zwally et al., 2002). In addition, Arctic sea ice extent has decreased from 1979 to 2006 in every month (Serreze et al., 2007). During the 2007 melt season, Arctic sea ice dropped to the lowest levels observed since satellite measurements began in 1979, resulting in the first recorded complete opening of the Northwest Passage (NSIDC, 2007). Arctic sea ice extent for 2008 was the second lowest on record (Figure 1) and was accompanied by the opening of the Northern Sea Route (NSIDC, 2008, http://nsidc.org/arcticseaicenews/index.html).
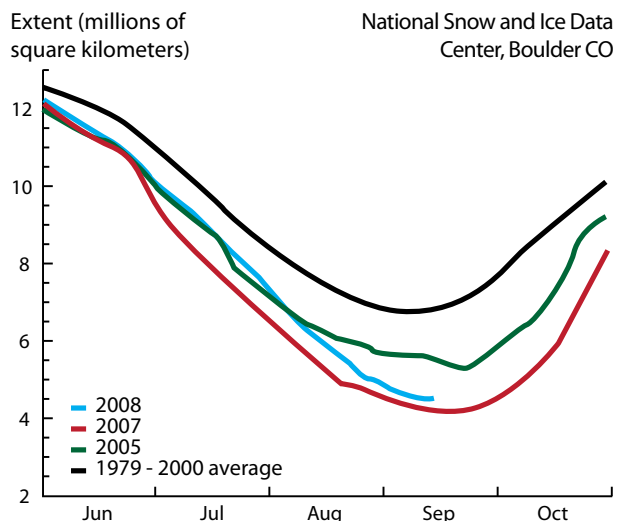

Figure 1. Daily sea ice extent. The blue line indicates 2008 extent, the grey line indicates extent for the average over 1979 to 2000, and the dotted green line shows extent for 2007 (National Snow and Ice Data Center).

Impacts of ice loss include reduction of the Earth's albedo, a positive feedback which leads to further warming. As the sun rises in the spring, temperatures increase, and snow on the surface begins to melt leading to the exposure of bare sea ice and, with continued melting, ocean water. Exposing the underlying dark surfaces leads to a decrease in albedo, an increase in the absorption of solar energy, and further warming. The result, a snow-albedo feedback, is one of the reasons that the Arctic is highly sensitive to changes in temperature. The earlier onset of spring melt observed in recent years is of particular concern as this is the season of maximum snow-albedo feedback (e.g., Hall and Qu, 2006).

Timescales for a collapse of the Greenland ice sheet and a transition to a seasonally ice-free Arctic are highly uncertain, as are the regional and global impacts. However, clear ecological signals of significant and rapid response to these changes within the Arctic are already present. For example, paleolimnological data from across the Arctic have recorded striking changes in diatoms and other bioindicators corresponding to conditions of decreased ice cover and warming (Smol et al. 2005). Circumpolar vegetation also is showing signs of rapid change, including an expansion of shrub and tree coverage (Chapin et al., 2005). An earlier snowmelt on land in arctic and alpine tundra will have direct and substantial impacts on plant primary production. A two-week prolongation of the growing season in May (when global radiation influx is at maximum) will potentially result in a 15-25% increase in productivity (whereas a similar prolongation in September/October has no effect as light quality is inferior for photosynthesis) (Björk and Molau, 2007). However, the major proportion of that increase in tundra plant biomass will be accounted for by invasive boreal species (e.g., birch, willow, blueberry, certain grasses), outcompeting the resident arctic specialist species (Sundqvist et al., 2008). This shift in plant biodiversity will have immediate negative impacts on animal biodiversity, which, in turn, implies large shifts in the lifestyle of indigenous peoples and for activities like tourism and reindeer husbandry. This ongoing "shrubbification" has already been documented to occur in the arctic and subarctic parts of Alaska and Scandinavia (Walker, 2006). Reduction in sea ice most likely also will be devastating for polar bears, ice-dependent seals, and people who depend on these animals for food (ACIA, 2004). Warming and melting of the Arctic will also impact the planet as a whole (ACIA, 2004) as melting of Arctic glaciers is one of the factors contributing to sea-level rise around the world.

Arctic warming is primarily a manifestation of global warming, such that reducing global-average warming will reduce Arctic warming and the rate of melting (IPCC, 2007). Reductions in the atmospheric burden of CO_2 are the backbone of any meaningful effort to mitigate climate forcing. But even if swift and deep reductions were made, given the long lifetime of CO_2 in the atmosphere, the reductions may not be achieved in time to delay a rapid melting of the Arctic. Hence, the goal of constraining the length of the melt season and, in particular, delaying the onset of spring melt, may best be achieved by targeting shorter-lived climate forcing agents, espe-

cially those that impose a surface forcing that may trigger regional scale climate feedbacks pertaining to sea ice melting. Examples of such forcings include tropospheric aerosols that impact radiative fluxes in the Arctic (e.g., Garrett and Zhao, 2006; Lubin and Vogelmann, 2006), the deposition of aerosols containing black carbon leading to enhanced absorption of radiation at the surface (e.g., Warren and Wiscombe, 1980; Flanner et al., 2007), and tropospheric ozone contributing to seasonal warming trends in the Arctic (Figure 2) (Shindell et al., 2006). Addressing these short-lived species (tropospheric aerosols, tropospheric ozone, and methane) has the advantage that emission reductions will be felt much more quickly than reductions of long-lived greenhouse gases.

The large uncertainties associated with parameterizing the forcing and temperature response due to these pollutants prevent us from providing definitive answers regarding impacts and mitigation strategies. We can, however, describe the mechanisms by which these short-lived pollutants impact Arctic climate, focus attention on the issues involved in estimating forcings and temperature responses and developing successful mitigation strategies, and provide initial seasonally averaged forcing and response estimates for the Arctic. In addition, we can outline near-term climate mitigation opportunities for the Arctic and recommend areas of future research that are required to reduce uncertainties in the forcing and temperature estimates.
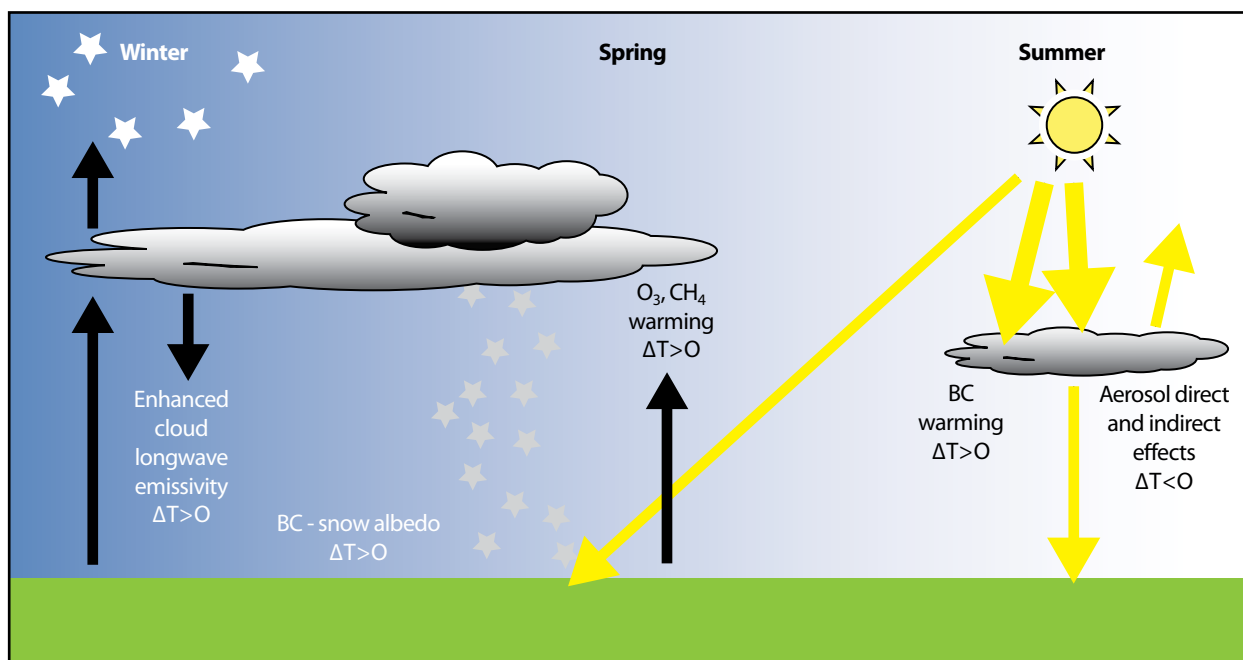
Figure 2. Forcing mechanisms in the Arctic due to short-lived pollutants. ΔT indicates the surface temperature response (Quinn et al., 2008).

2. Short-Lived Pollutants that Impact Arctic Climate

2.1 Transport of Pollutants to the Arctic

Surfaces of constant potential temperature form a closed dome over the Arctic that serve to isolate the Arctic lower troposphere from the rest of the atmosphere (Klonecki et al., 2003; Stohl, 2006). During the winter, the dome, also known as the Arctic front, can extend to as far south as 40°N over northern Europe and Asia (Figure 3). During the summer, the front is confined to a much smaller, higher latitude region.

Determining the relative importance of emissions from different source regions on levels of pollutants in the Arctic is required for the development of strategies to mitigate Arctic warming due to short-lived pollutants. Stohl (2006) developed a climatology of transport to the Arctic based on a Lagrangian particle dispersion model, resolved winds from European Centre for Medium-Range Weather Forecasts (ECMWF) analyses, and parameterized turbulent and convective transport. From the 5.5 year model run, three typical transport patterns were identified: 1) Rapid (4 days or less) low-level transport into the Arctic followed by uplift at the Arctic front. This route is possible from populated regions in Europe that are located at high enough latitudes to be north of the polar front. It also is a frequent transport

Figure 3. Warming in the Arctic since Pre-industrial Times, Quinn et al (2007). Best estimate of calculated temperature increase for deposited (surface) black carbon.

route from boreal forest fire regions into the Arctic (Stohl et al., 2006). This transport pathway may result in the deposition of particulates to the Arctic surface as the uplift and subse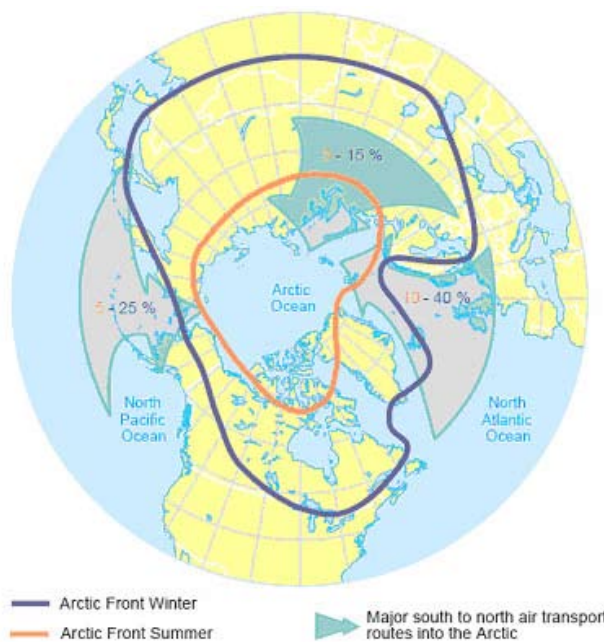quent precipitation occurs north of 70°N. 2) Low-level transport of cold air masses that cool even further as they travel over snow-covered surfaces into the polar dome (10 – 15 days). This route is possible from European and high-latitude Asian source regions as it involves transport over snow-covered high-latitude Siberia. It does not occur in the summer when surface temperatures over Eurasia are higher. 3) Ascent south of the Arctic near a source region followed by high-altitude transport and a descent into the polar dome due to radiational cooling. Stohl (2006) concludes that this is the only frequent transport route from North America and East Asia. Given the long transport time from pollution source regions in North America, South Asia, and East Asia relative to the atmospheric lifetime of aerosol particles and the potential for particle removal due to wet deposition, Stohl (2006) argues that European emissions have a much stronger impact on pollution levels at the Arctic surface. However, Stohl (2006) found that the contribution from European source regions decreases with altitude while the contribution from South Asian source regions increases with altitude.

In a separate study, global multi-model simulations performed as part of the Task Force on Hemispheric Transport of Air Pollution (HTAP) characterized the

relative importance of emissions from different source regions on pollution levels within the Arctic (Shindell et al., 2008). Source regions considered included Europe, North America, East Asia, and South Asia (Figure 4). A North Asian (Russian) source region was not included but Arctic sensitivities to this region's emissions are expected to be similar to that of the European region given their proximity and similar meteorological conditions.

Figure 4. The four source regions (shaded) considered in the HTAP study (Shindell et al., 2008).

Based on the emission inventories used by each model and calculated Arctic sensitivities (change in mixing ratio per unit emission), the largest total contribution to the annual average abundance of aerosol sulfate and BC at the Arctic surface was found to be from Europe (Figure 5). In addition, Europe was the dominant contributor to the abundance of sulfate and BC at the surface on a seasonal basis, i.e., it was largest contributor during winter, spring, summer, and fall. In the upper troposphere (250 hPa), abundances of sulfate and BC were found to be dominated by Asian emissions (South + East) on both an annual and seasonal basis. The situation in the mid-troposphere (500 hPa) was found to be more complex. European emissions dominated the sulfate abundance annually and in all seasons. For BC, Asian emissions (South + East) were found to dominate during spring, be comparable to European emissions in winter and fall, and be slightly less than European emissions during summer. Arctic O_3 levels were reported to have less variation in regional sensitivity as a function of altitude; they were most responsive to North American NO_x emissions at all levels.

The Stohl (2006) and Shindell et al. (2008) studies both reported that European emissions had the largest impact on aerosol sulfate and BC abundances at the Arctic surface. In addition, both found that Asian emissions had an impact at higher altitudes with Shindell et al. (2008) estimating a much larger contribution from Asia, especially for BC. The difference can not be attributed to emissions as both studies used similar emission inventories. Shindell et al. (2008) suggests that the discrepancy may be a result of fundamental differences in the model approach used in the analyses. In any case, it is clear that European emissions have a large impact on aerosol sulfate and BC at the Arctic surface, Asian emission become more important with increasing altitude, and North America dominates the abundance of O_3 at all altitudes within the Arctic.

2.2 Methane

Sources and trends. Since the industrial revolution, rapid increases in human activity have led to more than a doubling of atmospheric methane concentrations (Wuebbles and Hayhoe, 2002). A combination of ice core records and atmospheric measurements has revealed that methane levels, at ~ 1770 ppb, are higher now than at any time in the past 650 kyr (Petit et al., 1999; Spahni et al., 2005). Growth rates have slowed over the last few decades with current observations indicating that methane levels are either leveling off or starting to increase after a brief decline in the early 1990s (Figure 6) (Dlugokencky et al., 2003). At the same time, growth rates are becoming more variable. Methane emissions are expected to increase in the future due to increases in fossil fuel use and
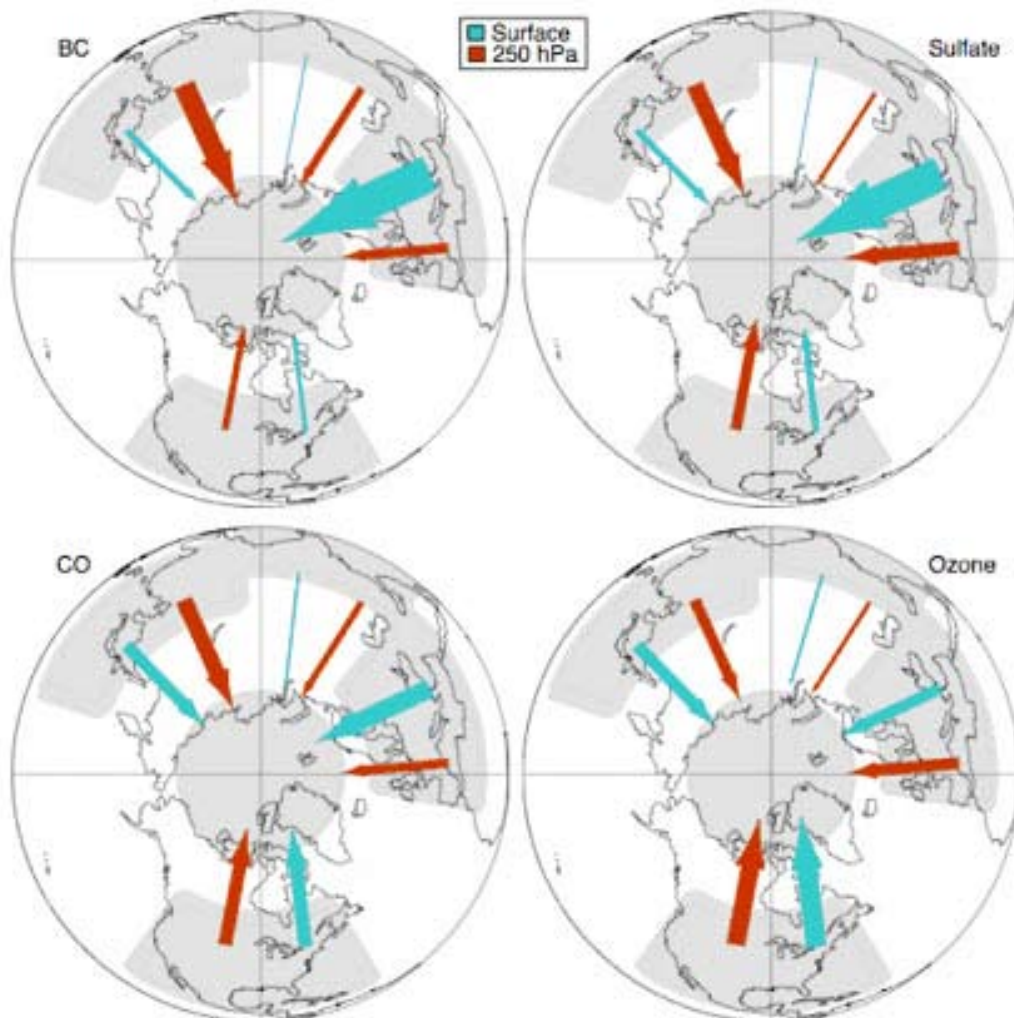
Figure 5. Relative importance of source regions to annual mean Arctic concentrations at the surface and in the upper troposphere (250 hPa) for the indicated species. Values are calculated from simulations of the response to 20% reduction in anthropogenic emissions of precursors from each region (using NO_x for ozone). Arrow width is proportional to the multimodel mean percent contribution from each region to the total from these four source regions (Shindell et al., 2008).

perhaps as a result of changes in wetlands at high latitudes due to increasing temperatures (Bruhwiler and Matthews, 2007).
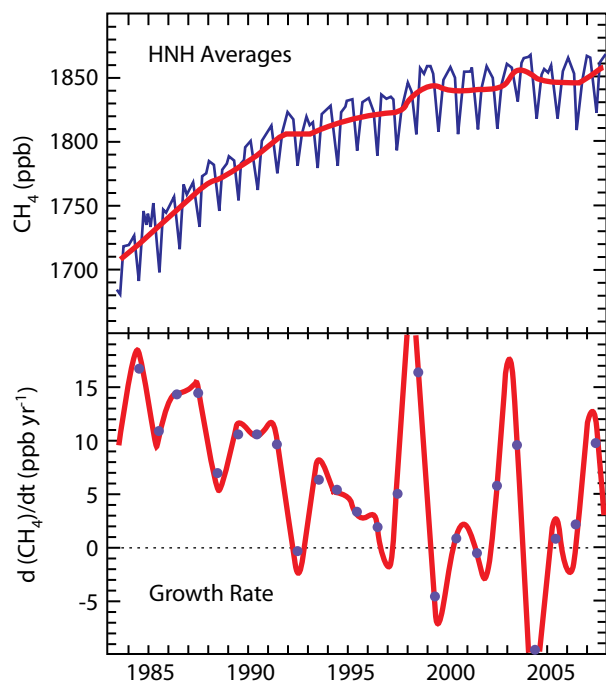
Figure 6. High northern hemisphere (53°N to 90°N) average concentrations of methane from the NOAA air sampling network since 1983. Shown are (top) the de-seasonalized high northern hemisphere trend and weekly averages and (bottom) the derivative with respect to time with uncertainties (± 1σ, daished line) and annual increases (Courtesy E. Dlugokencky, NOAA/ESRL).

Anthropogenic sources, which account for about two thirds of emitted methane, include coal and gas production and use, rice cultivation, solid waste from animals, waste disposal, biomass burning, landfills, and enteric fermentation (e.g., Kirchgessner, 2000; Huang et al., 1998; Harper et al., 1999; Houweling et al., 1999; Johnson et al., 2000). The largest single source of methane is natural wetlands (IPCC, 2001) with wetlands north of 60°N responsible for about 13% of the global natural methane flux (Cao et al., 1998). Arctic wetland ecosystems convert part of the carbon that has been photosynthetically captured from the atmosphere in the form of CO_2 to methane. Measurements in the sub-Arctic and Arctic over the past decade have indicated that methane emissions from these regions are increasing due to increasing temperatures and the resulting disappearance of permafrost and wetter soil conditions (e.g., Nakano et al., 2000, Zimov et al., 2006). Permafrost and vegetation changes in one region in sub-Arctic Sweden have led to 20 to 70% increases in local methane emissions between 1970 and 2000 (Christensen et al., 2004). In Arctic regions of continuous permafrost, warming has resulted in a degra-

dation of permafrost and an increase in the size and number of thaw lakes. It has been estimated that this increase in lake area has led to a 58% increase in methane emissions from thermokarst lakes near the Kolyma Rvier, from 2.4 to 3.8 Tg of CH_4, between 1974 and 2000 (Walter et al., 2006). Further warming in Siberia could result in thousands of teragrams of methane being emitted from the 500 gigatons of labile C that is currently stored in regional permafrost. (By comparison, the atmosphere now contains 5000 teragrams of methane.).

Radiative forcing. With a lifetime of about 9 years (Prinn et al., 1995), methane is much shorter lived than CO_2 but still is globally well-mixed. Methane has contributed the second largest anthropogenic radiative forcing since the pre-industrial after CO_2 and, on a per molecule basis, is a more effective Greenhouse Gas (GHG) than CO_2 (IPCC, 2001). Radiative forcing by methane results directly from the absorption of longwave radiation and indirectly through chemical reactions that lead to the formation of other radiatively important gases (Wuebbles et al., 2002). The latter is dominated by the formation of tropospheric ozone, also a short-lived GHG, through the oxidation of methane by the hydroxyl radical (OH) in the presence of nitrogen oxides (NO_x) and sunlight. Radiative forcing due to globally-well-mixed methane contributes to Arctic warming as the climate system transports heat from distant regions to the Arctic. Global warming is amplified in the Arctic due to the snow-albedo feedback discussed above.

2.3 Tropospheric Ozone

Sources and trends. Both observations and modeling studies provide evidence that tropospheric ozone concentrations, which are controlled primarily by photochemical production and loss processes within the troposphere, have increased since pre-industrial times due to increases in emissions of anthropogenic ozone precursors (Oltmans et al., 1998). The rapid increase in ozone concentrations during the latter half of the 20th century has been attributed to increases in economic development at middle and low latitudes (Shindell et al., 2006). Tropospheric ozone is formed in the atmosphere from precursor gas phase species in the presence of light. The precursors include NO_x, carbon monoxide, methane, and non-methane volatile organic compounds (NMVOC) (Haagen-Smit (1952); Seinfeld (1988)). Anthropogenic sources of these precursor gases include fossil fuel combustion and production, biofuel combustion, industrial processes, and anthropogenic biomass burning. Natural sources include wild-

fires, biogenic emissions from soils and vegetation, and lightning.

In polluted air masses, ozone is formed primarily from rapid photochemical oxidation of NMVOCs in the presence of NO_x (e.g., Chameides et al., 1992). In contrast, methane, being globally well-mixed, contributes to increases in background tropospheric ozone levels (Crutzen, 1973; Fiore et al., 2002; Dentener et al., 2005). The lifetime of ozone decreases during the summer in the extratropics since photochemical destruction rates increase with increasing insolation (Shindell et al., 2006). The atmospheric lifetime of ozone is roughly days to weeks in summer and 1 to 2 months in winter. Hence, ozone that is produced in the northern hemisphere mid-latitudes is most efficiently transported to the Arctic in the non-summer months.

Radiative forcing. Changes in local tropospheric ozone affect Arctic climate by altering local radiation fluxes. Little is known, however, about the contribution of local production of ozone and its precursors within the Arctic relative to extrapolar sources. Local sources include marine vessel emissions which are expected to increase as sea ice decreases in the coming years. It has been estimated that shipping emissions in the Arctic have the potential to increase Arctic ozone levels by a factor of 2 to 3 in the decades ahead relative to present day levels (Granier et al., 2006).

Sub-Arctic and Arctic ozone precursor emissions may be increasing as boreal regions warm and forest fire frequency increases (Kasischke et al., 2005). Fires emit large quantities of CO and non-methane volatile organic carbon (NMVOC) compounds which may combine with anthropogenic emissions in the same region to produce large amounts of ozone. Generoso et al. (2007) showed that CO emissions from boreal fires in the spring and summer of 2003 made a substantial impact on O_3 concentrations in the Arctic. Agricultural fires may be particularly important sources to the Arctic, especially in eastern Europe and northern Asia as these are regions with very high fire frequency (Korontzi et al., 2006).

Record high concentrations of ozone were measured at the Zeppelin research station in Spitsbergen (79°N) in April and May of 2006 (Stohl et al., 2007). This severe air pollution episode was a result of the combination of unusually high temperatures in the European Arctic and large emissions from agricultural fires in Belarus, Ukraine, and Russia (Figure 7). The high temperatures in the Arctic reduced the temperature gradient between the source and receptor regions, making low-level transport of pollution into the Arctic possible. Should the warming of the Arctic continue to proceed more quickly than that of the middle latitudes, transport from highly polluted source regions

may become more frequent in the future, resulting in increased tropospheric ozone concentrations and a further increase in surface temperatures.

Figure 7. View from the Zeppelin research station during the spring 2006 smoke event. Image courtesy of Ann-Christine Engvall (Stohl et al., 2007).

Based on a series of climate model simulations, Shindell (2007) demonstrated a strong correlation between local forcing within the Arctic and Arctic surface temperature response during summer. Hence, ozone produced by summertime boreal forest fires may have a significant impact on Arctic surface temperatures.

Changes in distant (extrapolar) ozone amounts can affect the heat that is available to be transported to the Arctic. Shindell (2007) demonstrated that, during non-summer seasons, the local radiative forcing from ozone is not a good metric for estimating the surface temperature response in the Arctic. Rather, the Arctic surface warms during the non-summer seasons in response to a remote forcing (either global or northern hemisphere extratropical) which is positive due to increased tropospheric ozone. As Shindell (2007) points out, this result does not mean that local forcing does not influence the Arctic but, that for the historical changes in concentrations of short-lived pollutants included in the model runs, the remote forcing dominates over the local especially during the time of year when the snow-albedo feedback is at a maximum.

2.4 Tropospheric Aerosols

Sources and trends. Arctic haze is detected each year as a large increase in tropospheric aerosol concentrations in late winter and early spring (e.g., Shaw, 1995; Sirois and Barrie, 1999) (Figure 8). The combination of intense isentropic transport from the mid-latitudes to the Arctic and strong surface-based

temperature inversions that inhibit turbulent transfer (and, therefore, aerosol removal via deposition) results in this recurring phenomenon (Iversen and Joranger, 1985; Klonecki et al, 2003). In addition, the dryness of the Arctic troposphere yields very little wet deposition during this time of year which can result in very long aerosol lifetimes (Shaw, 1981).
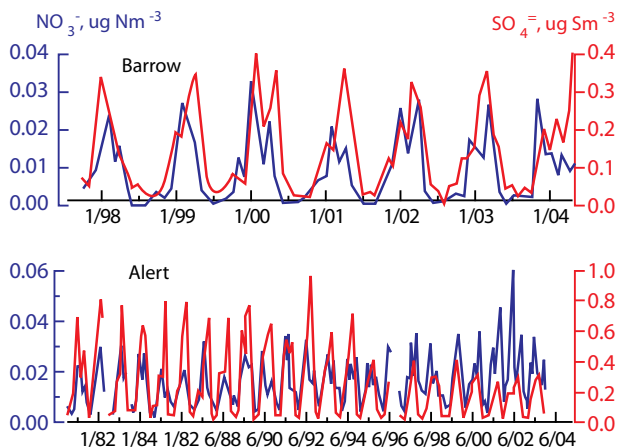

Figure 8. Time series of monthly averaged particulate sulfate and nitrate concentrations at Barrow, Alaska (top) and Alert, Canada (bottom) showing increase in concentrations during winter and early spring (Quinn et al., 2007). Data made available for Alert by the Canadian National Atmospheric Chemistry (NAtChem) Database and Analysis System and for Barrow by NOAA PMEL (http://saga.pmel.noaa.gov/data/).

Long-term, ground-based measurements of sulfate and light scattering by aerosols show that, since the late 1970s, the highest recorded levels of Arctic Haze occurred in the 1980s and early 1990s (Quinn et al., 2007). Levels then decreased through the end of the 1990s primarily due to reductions in industrial emissions in the early years of the new Eurasian republics and, to a lesser extent, to more stringent power plant emission laws in the United States and Europe. More recent measurements indicate that levels of light scattering and black carbon may be increasing once again (e.g., Sharma et al., 2006). From 1980 to the present, nitrate concentrations have increased, suggesting that while power-plant sulfur emissions have decreased in the source regions to the Arctic, emissions from diesel and gasoline engines have increased (Figure 9) (Quinn et al., 2007). The same agricultural fire event reported by Stohl et al. (2007) that resulted in anomalously high ozone also led to record high levels of aerosol optical depth and black carbon, indicating the potential impact of natural and prescribed episodic fires.

Radiative forcing. Tropospheric aerosols in the Arctic can perturb the radiation balance of the earth-atmosphere system in a number of ways (Quinn

et al., 2007). Direct aerosol forcing occurs through absorption or scattering of solar (shortwave) radiation by aerosols. For example, a scattering aerosol over a low albedo surface will reflect incoming solar radiation, resulting in a cooling of the surface as well as the surface-atmosphere-aerosol column. An absorbing aerosol, such as one containing soot (BC), over a highly reflective surface will result in a warming at altitudes above and within the haze layer and, instantaneously, a reduction of solar energy at the surface (Shaw and Stamnes, 1980). The added atmospheric heating will subsequently increase the downward longwave radiation to the surface, warming the surface. With the highly reflective surfaces typical of the Arctic springtime, even a moderately absorbing aerosol can lead to a heating of the surface-atmosphere-aerosol column. The Airborne Arctic Stratospheric Expedition (AASE) II flights in the winter of 1992 observed soot-containing aerosols at an altitude of 1.5 km. Pueschel and Kinne (1995) calculated that this layer of aerosols could heat the earth-atmosphere system above a surface of high solar albedo (ice/snow) even for single-scattering albedos as high as 0.98.
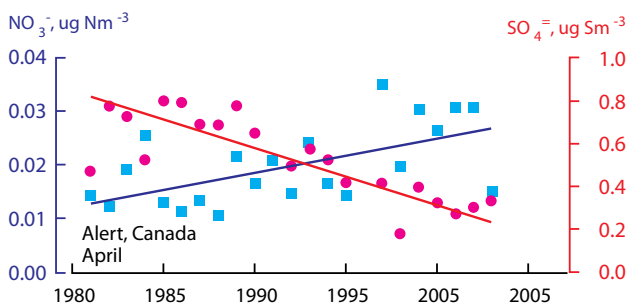
Figure 9. Monthly averaged concentrations of nitrate and sulfate for April at Alert, Canada. The solid line indicates the Sen's slope estimate for the long term trend and indicates the decrease in sulfate due to lowered power plant emissions and the increase in nitrate to due more emissions from diesel and gasoline engines (Quinn et al., 2007). Data made available for Alert by the Canadian National Atmospheric Chemistry (NAtChem) Database.

If hygroscopic pollution particles deliquesce and grow sufficiently large they may also impact the radiation balance in the Arctic by interacting with terrestrial (longwave) radiation (MacCracken et al., 1986). This forcing may be significant during the polar night when longwave radiation dominates the energy budget. Measurements made in the Arctic when the sun was below the horizon suggest that Arctic haze can have a detectable direct thermal radiative forcing by altering the flux of both downward and outgoing longwave radiation (Ritter et al., 2005).

Soot has an additional forcing mechanism, referred to as BC-snow forcing, when it is deposited to snow and ice surfaces (Clarke and Noone, 1985). Such deposition darkens the surface which enhances absorption of solar radiation thereby warming the lower atmosphere and inducing snow and ice melting. Shindell et al. (2008), as part of the HTAP study discussed in Section 2.1, investigated the relative importance of the various source regions to BC deposition to Greenland and the rest of the Arctic (Figure 10). They found that deposition of BC to the Arctic (excluding Greenland) was most sensitive to emissions from Europe in every season. On an annually averaged basis, 68% of the BC deposited to the Arctic (excluding Greenland) originated from Europe, 11% from North America, and 22% from Asia (South + East).

Deposition of BC to Greenland is more sensitive to emissions from North America than the rest of the Arctic because of its high topography which allows inflow of air from warmer source regions (Stohl, 2006). On an annual basis, models estimated that both North American and European source regions

contribute about 40% to the BC deposited to Greenland while Asian regions (South and East) contribute about 20%. The relative importance changes as a function of season, however. Shindell et al. (2008) found that total springtime deposition to Greenland is primarily due to emissions from North America and East Asia. BC deposited in the spring is expected to be most effective in enhancing snow-albedo feedbacks (Flanner et al., 2007). Hence, North American and East Asian emissions may have a stronger role in Greenland climate forcing than is indicated by their annual mean contribution to deposition.

The Shindell et al. (2008) study did not include emissions for North Asian (Russian) source regions which most likely make a significant contribution to the BC deposited in the Arctic, especially outside of Greenland.

In addition to the modeling studies described above, measurements of BC and other tracer species in central Greenland ice cores have been used to determine the concentrations and sources of BC in snow and to estimate the impact of BC on radiative forcing on the Greenland ice sheet and the Arctic

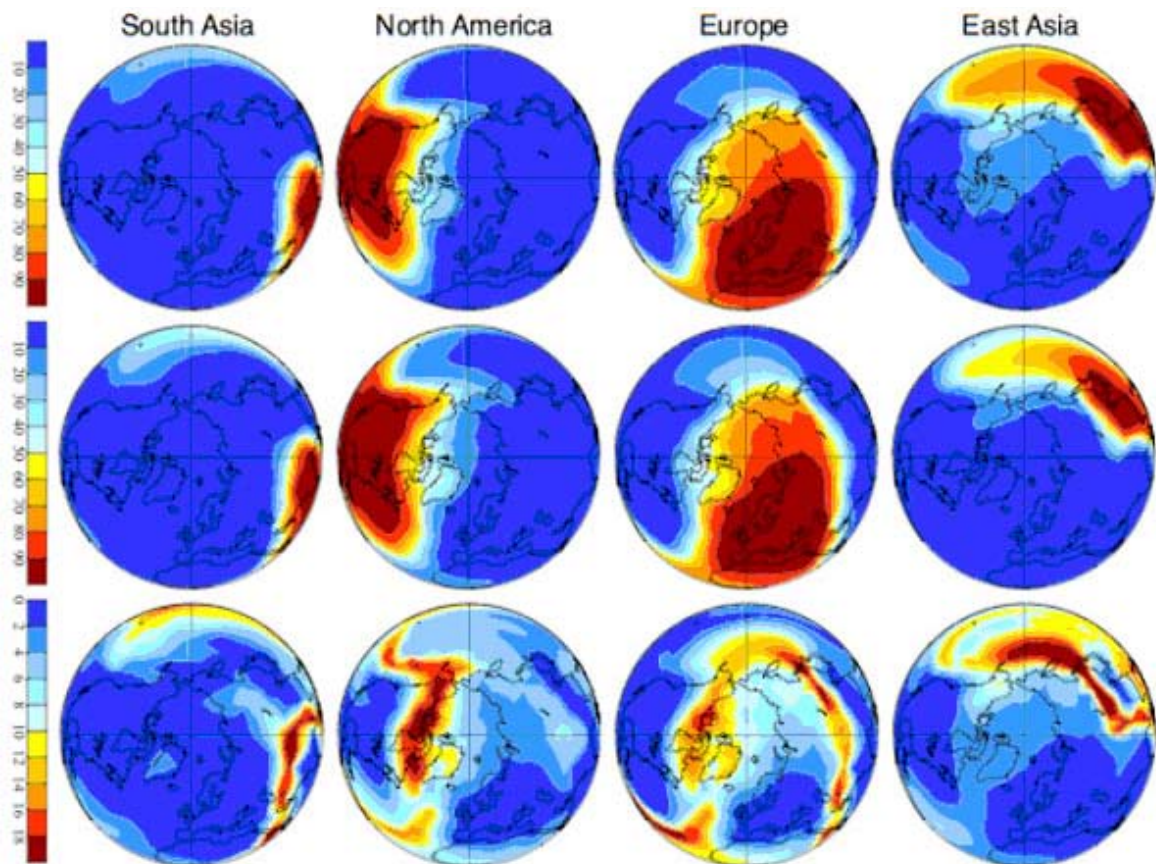Figure 10. Relative contribution or regional emissions to winter Arctic surface BC (which is strongly correlated with, and therefore illustrative of, BC deposition). Relative contribution (%) to the total response to emissions from the four source regions (left), the relative contribution (%) per unit source region emission (center), and the standard deviation of the latter across all HTAP models (right) (Shindell et al., 2008).

over the past 215 years (McConnell et al., 2007). Chemical analyses combined with air mass back-trajectory modeling indicate that eastern North American boreal forest fires were likely the major source of BC in Greenland precipitation prior to industrialization (~1850) and a significant source throughout the 215 year record. Since 1850, the BC deposited to Greenland snow appears to have originated primarily from industrial activities in North America (1850 – 1950) and Asia (1950 – present). Because of their short (~3 day) atmospheric lifetimes, concentrations and deposition fluxes of BC and other tropospheric aerosols are highly variable in space and time. It is likely that these first results from Greenland are representative only of the North Atlantic region of the Arctic that is strongly influenced by North American and Western European emissions.

In years of intense burning, boreal forest fires can be an important source of BC to the atmosphere throughout the Arctic. Stohl et al. (2006) found Pan-Arctic enhancements of aerosol light absorption during the summer of 2004, a year with strong burning in Canada and Alaska. Measurements of BC in snow at Summit confirm the deposition of BC to the snow surface. The summer of 2004 stands out as having the highest BC concentrations in snow in recent years (Hagler et al., 2007) yet the range of concentrations (1.0 – 1.4 ng g-1) was far too low to significantly affect snow albedo if the BC were uniformly distributed in the upper snow layers (Warren and Wiscombe, 1985, Figure 2). A thin layer of BC on the top surface might reduce albedo until it is covered with new snow. However, even if the snow albedo at Summit is usually unaffected by BC, this does not rule out a significant effect at lower-elevation locations in the Arctic, where average BC concentrations are usually much larger. Boreal forest fires in Siberia may have a larger impact than those in North America because of the larger burn area (Stohl, 2006). The fires occurring in Siberia in 2003 have been estimated to account for 16 to 33% of the observed aerosol optical thickness and 40 to 56% of the mass of BC deposited north of 75°N in spring and summer (Generoso et al., 2007).

Once BC has been deposited to glaciers, it has lasting impacts. First, BC deposited directly on glacier ice tends to remain for years before being removed by surface run-off processes. Field studies have shown that the accumulation of aerosols far exceeds annual deposition rates of aerosols. Second, BC entrained in snow accumulation on large glaciers and ice caps is gradually buried and is transported downward due to ice flow. It is this ice flow and, hence, preservation of atmospheric signals that enabled McConnell et al. (2007) to document the

history of emissions of BC to the Arctic. The ice flow will eventually transport the ice-entrained BC down and out to the melt zone of the ice sheet where free melt of BC on the Greenland ice sheet will release BC in the centuries or perhaps millennia to come.

Climate forcings also result from aerosol-cloud interactions. The aerosol first indirect effect in the shortwave occurs when pollution particles lead to an increase in cloud droplet number concentration, a decrease in the size of the droplets, and a corresponding increase in shortwave cloud albedo (Twomey, 1977). Measurements made at Barrow, Alaska, over a four year period indicate that episodic Arctic Haze events produce high cloud drop number concentrations and small cloud drop effective radii in low-level cloud microstructures (Garrett et al., 2004). Similar aerosol-cloud interactions can also lead to a significant longwave forcing. When the cloud drop number concentration of thin Arctic liquid-phase clouds is increased through interaction with anthropogenic aerosols, the clouds become more efficient at trapping and re-emitting longwave radiation (Garrett and Zhao, 2006; Lubin and Vogelmann, 2006). Over dark oceans when the sun is high, the shortwave indirect effect is expected to cool the surface but for a low sun over bright Arctic surfaces, the longwave effect is expected to dominate. Lubin and Vogelmann (2007) performed radiative transfer simulations to assess the relative magnitudes of shortwave and longwave downwelling fluxes due to Arctic haze aerosols. During March and April, shortwave downwelling fluxes were found to be comparable in magnitude to longwave fluxes. During May and June, however, the shortwave fluxes exceeded those in the longwave.

Aerosol-cloud interactions may also increase cloud cover by increasing cloud droplet number concentrations. The result is a decrease in cloud drop size, a decrease in precipitation, and an increase in cloud lifetime (Albrecht, 1989). Finally, increasing cloud drop number concentrations may be associated with a reduced rate of ice formation in mixed-phase Arctic clouds which reduces cloud desiccation by ice and increases cloud longwave emissivity (Girard et al., 2005). However, ice formation mechanisms in common mixed-phase clouds remain very poorly understood (Fridlind et al., 2007).

2.4 Summary of the Forcing due to Short-Lived Pollutants

Surface temperature responses are strongly linked to surface radiative forcings in the Arctic because the stable atmosphere of the region prevents rapid heat exchange with the upper troposphere (Hansen

and Nazarenko, 2004). In turn, the magnitude of the forcing by each short-lived pollutant depends on the seasonality of a number of inter-related factors including radiation, precipitation, surface albedo, snow and ice coverage, and pollutant transport. In Section 3, estimates are presented of seasonally averaged forcing and the surface temperature response for the short-lived pollutants. Although average estimates of temperature response may not be the most informative measure of the impact of short-lived pollutants, they serve as a starting point and can indicate directions for future research and mitigation strategies.

3. Methods

Radiative forcings and temperature response values for methane, tropospheric ozone, and tropospheric aerosols are presented so that the impact of these individual forcing agents can be compared in terms of seasonality, forcing at the surface (FS), forcing at the top of atmosphere (FTOA), and surface temperature response (ΔTS).

Methods used to estimate seasonally averaged radiative forcings and temperature responses due to the short-lived pollutants are described below and summarized in Tables 1 and 2. These calculations and results were first presented in Quinn et al. (2008).

3.1 Surface and top of atmosphere forcing

Seasonally averaged values of FS, FTOA, and FTOA – FS for the short-lived pollutants are shown in Table 3. Values of FS and FTOA due to direct radiative forcing by tropospheric aerosols are based on GISS ModelE GCM calculations (Koch and Hansen, 2005). They are reported as the change in instantaneous forcing due to adding present-day fossil fuel plus biofuel emissions to the baseline simulation where the baseline simulation used present-day biomass burning emissions. For comparison, values also are shown for the forcing contributed by present-day biomass burning emissions based on GISS ModelE GCM calculations.

Table 1. Description of the calculation of seasonally averaged forcing for the Arctic (60°N to 90°N) calculated as the change in instantaneous forcing due to the addition of fossil and biofuel emissions to present day biomass burning emissions.

Forcing	Method	Output
Tropospheric Aerosols		
Direct Effect $SO_4^= + OC + BC$ **Indirect Effect** (Cloud cover and albedo) $SO_4^= + OC + BC$	GISS ModelE GCM. Global scale calculation. Forcings averaged over the Arctic. Present day fossil, biofuel, and biomass burning emissions relative to present day biomass burning.	F_S and F_{TOA} Averaged over the Arctic
Cloudwave longwave emissivity	Measurements of the sensitivity of low-level cloud emissivity to pollution at Barrow, AK. Not a seasonal average.	F_S for when low-lying clouds and aerosols are coincident.
BC-snow albedo	SNICAR (radiative transfer calculations) coupled to NCAR CAM3 GCM. Global scale calculation. Forcings averaged over the Arctic. Present day fossil, biofuel, and biomass burning emissions relative to present day biomass burning.	F_S Averaged over the Arctic.
Tropospheric O_3		
GHG warming + shortwave absorption	GISS Model II. Global scale calculation. Forcings averaged over the Arctic. 1880 – 2003 time period. Fossil, biofuel, and biomass burning.	F_{TOA} Averaged over the Arctic.
Methane		
GHG warming	GISS Model II GCM. Global scale calculation. Forcings averaged over the Arctic. 1900 - 2001 time period. Driven by changes in all WMGHGs accounting for the contribution of CH_4 to total forcing (0.2) and its efficacy relative to the total (1.05/1.02).	F_{TOA} Averaged over the Arctic.

Table 2. Description of the estimation of seasonally averaged surface temperature response for the Arctic (60°N to 90°N) to forcings due to the short lived pollutants.

Forcing	Method	Output
Tropospheric Aerosols		
Direct Effect $SO_4^= + OC + BC$	GISS ModelE GCM. Zonal mean temperature change averaged over the Arctic in response to the global forcing.	ΔT_S (°C) averaged over the Arctic.
Indirect Effect (Cloud cover effect only) $SO_4^= + OC + BC$		
Cloudwave longwave emissivity	Based on measurements of the sensitivity of low-level cloud emissivity to pollution at Barrow, AK.	ΔT_S (°C) for when low-lying clouds and aerosols are coincident.
BC-snow albedo	SNICAR coupled to NCAR CAM3 GCM.	ΔT_S (°C) averaged over the Arctic.
BC-atmospheric warming	1 W m⁻² = 0.15 °C (IPCC, 2007).	ΔT_S (°C) averaged over the Arctic.
Tropospheric O_3		
GHG warming + shortwave absorption	GISS Model II. Zonal mean temperature change averaged over the Arctic in response to the global forcing.	ΔT_S (°C) averaged over the Arctic.
Methane		
GHG warming	GISS Model II GCM. Zonal mean temperature change averaged over the Arctic in response to the global forcing.	ΔT_S (°C) averaged over the Arctic.

Table 3. Comparison of the seasonality and magnitude of the forcing as well as the surface temperature response due to short-lived pollutants in the Arctic (60° to 90°N). Values of FS and FTOA are reported here as the change in the instantaneous forcing due to the addition of fossil fuel and biofuel emissions to present-day biomass burning emissions. Winter = DJF, Spring = MAM, Summer = JJA, Fall = SON.

Forcing Agent	Season	F_S, W m⁻²	F_{TOA}, W m⁻²	F_{TOA-S}, W m⁻²	ΔTs[a], °C
Tropospheric Aerosols - Direct Effect[b]					
Total* Fossil+Bio Fuel (Biomass Burning) *$SO_4^= + OC + BC$	Winter	-0.04 (-0.001)	0.08 (0.004)	0.12 (0.005)	-1.4[c]
	Spring	-0.72 (-0.1)	0.92 (0.17)	1.6 (0.27)	-0.93[c]
	Summer	-0.93 (-0.43)	0.11 (0.16)	1.0 (0.59)	-0.47[c]
	Fall	-0.14 (-0.07)	0.08 (0.04)	0.22 (0.11)	-1.1[c]
$SO_4^=$ Fossil Fuel	Winter	-0.006	-0.01	-0.006	
	Spring	-0.26	-0.32	-0.06	
	Summer	-0.50	-0.54	-0.04	
	Fall	-0.07	-0.08	-0.01	
OC Fossil+Bio Fuel (Biomass burning)	Winter	-0.003 (0)	0 (0)	0.003 (0)	
	Spring	-0.06 (-0.05)	0.03 (0.02)	0.09 (0.07)	
	Summer	-0.04 (-0.24)	-0.01 (-0.09)	0.03 (0.15)	
	Fall	-0.008 (-0.04)	-0.001 (-0.02)	0.007 (0.02)	
BC Fossil+Bio Fuel (Biomass burning)	Winter	-0.03 (-0.001)	0.09 (0.004)	0.12 (0.005)	0.02[d]
	Spring	-0.39 (-0.05)	1.2 (0.15)	1.6 (0.20)	0.24[d]
	Summer	-0.39 (-0.19)	0.66 (0.25)	1.0 (0.44)	0.15[d]
	Fall	-0.07 (-0.03)	0.16 (0.05)	0.23 (0.08)	0.03[d]
Tropospheric Aerosols - Indirect Effects					
Total* Fossil+Bio Fuel Cloud albedo + cloud cover SW, LW, SW+LW *$SO_4^= + OC + BC$	Winter	-0.04, 0.24, 0.2[e]	0.07, -0.1, -0.03[f]	0.11, -0.34, -0.23	-0.77[g]
	Spring	-3.0, 1.9, -1.1	0, 0.1, 0.1	3.0, -1.8, 1.2	-0.68[g]
	Summer	-12.2, -0.5, -13	6.6, -0.5, 6.1	19, 0, 19	-0.45[g]
	Fall	-0.4, -0.1, -0.5	0.49, -0.9, -0.41	0.89, -0.8, 0.09	-0.89[g]
Cloud longwave emissivity	Winter	+3.3 to 5.2[h]			1 to 1.6[h]
Black carbon aerosol- Snow Albedo					
BC Fossil+Bio Fuel	Winter	0.02[i]			0.27-0.61[i]
	Spring	0.53[i]			0.36-0.76[i]
	Summer	0.21[i]			0.24-0.59[i]
	Fall	0.002[i]			0.31-0.76[i]
Tropospheric Ozone – GHG warming + SW absorption[j]					
O_3 Fossil+Bio Fuel and Biomass burning	Winter		0.13		0.43
	Spring		0.34		0.31
	Summer		0.14		0.11
	Fall		0.24		0.26

Table continued on next page.

Table continued from previous page.

Methane – GHG warming[k]					
Methane	Winter		0.29		0.34
	Spring		0.45		0.27
	Summer		0.55		0.15
	Fall		0.34		0.35

[a]Zonal mean temperature change at the surface for 60° to 90°N. Climate models used to calculate the Arctic response were forced globally (not just within the Arctic region) with changing composition.

[b]FS and FTOA are based on the GISS ModelE GCM, using present-day fossil, bio-fuel, and biomass burning emissions relative to present-day biomass burning emissions (Koch and Hansen, 2005). Values for present-day biomass burning emissions are shown in parentheses.

[c]Values are reported as the zonal mean temperature change for 1880 to 2003 at the surface relative to half present-day biomass burning emissions. Biofuel emissions are not included in these calculations. A small fossil fuel source was included for the late 1880s. Taken from Figure 11 of Hansen et al. (2007).

[d]Calculated from FTOA-FS for BC fossil and biofuel and assuming 1 W m^{-2} = 0.15°C (IPCC, 2007).

[e]Direct plus indirect effects (cloud albedo and cloud cover) together. Based on the GISS ModelE GCM, using present-day fossil, bio-fuel, and biomass burning emissions relative to present-day biomass burning emissions (Menon and Rotstayn, 2006). Three values are given: shortwave, longwave, and shortwave plus longwave forcing.

[f]Based on the GISS ModelE GCM, for changes in net cloud radiative forcing using the same emissions scenario as described above. Three values are given: shortwave, longwave, and shortwave plus longwave forcing.

[g]Temperature change due to cloud cover aerosol indirect effect only. Taken from Figure 11 of Hansen et al. (2007).

[h]Based on measurements of the sensitivity of low-level cloud emissivity to pollution at Barrow, Alaska (Garrett and Zhao, 2006). Not a seasonal average as it only includes times when pollution aerosol and clouds were coincident.

[i]Based on radiative transfer calculations with SNICAR coupled to the NCAR CAM3 using present-day fossil, bio-fuel, and biomass burning emissions relative to present-day biomass burning emissions (Flanner et al., 2007).

[j]Ozone forcing calculated at the tropopause over 60 - 90°N for 1900 - 2000 (Shindell et al., 2006).

[k]Methane's forcing and response are estimated based on simulations for 1900-2001 driven by changes in all well-mixed greenhouse gases (WMGHGs), accounting for the fractional contribution of methane to the total forcing (0.20) and its efficacy relative to the total WMGHG efficacy (1.05/1.02). As the well-mixed greenhouse gases are evenly distributed, we believe this is a realistic approach. Values are calculated at the tropopause.

Methane's role in ozone production is included in the tropospheric ozone calculation. Based on the contribution to the global increase in tropospheric ozone, it is responsible for ~50% of the overall tropospheric ozone increase. Its percentage contribution to the Arctic ozone concentration will be lower, however, as ozone changes in the Arctic are dominated by increases in NO$_x$ (Shindell et al., 2005).

FS and FTOA were calculated for the "total" aerosol which includes sulfate, organic carbon (OC), and black carbon (BC) and for the individual aerosol species (sulfate, OC, and BC). Forcings derived from these global-scale calculations were averaged over 60°N to 90°N.

Values of FS and FTOA due to indirect radiative forcing by tropospheric aerosols are based on GISS ModelE GCM calculations for direct plus indirect effects where the indirect effects include those of cloud albedo and cloud cover (e.g., Menon and Rotstayn, 2006). Shortwave, longwave, and shortwave plus longwave values of FS and FTOA are given for the "total" aerosol (sulfate, OC, and BC). As for the direct radiative forcing calculations, forcings are reported as the change in instantaneous forcing due to adding fossil fuel plus biofuel emissions to the baseline simulation where the baseline simulation used present-day biomass burning emissions.

Increased cloud longwave emissivity due to pollution haze is assigned a wintertime range of values of FS based on the analysis of Garrett and Zhao (2006). Using four years of ground-based aerosol and radiation measurements, Garrett and Zhao (2006) found that where thin water clouds and pollution are coincident, there is an increase in cloud longwave emissivity resulting from haze layers at altitudes above the surface. Rather than seasonal averages, the range of observed sensitivity and corresponding surface temperature response are reported here.

Forcing by BC in snow due to present-day fossil, bio-fuel, and biomass burning emissions for the Arctic (60° to 90°N) was calculated relative to present-day biomass burning emissions using SNICAR (Snow, Ice, and Aerosol Radiative model) coupled to

the NCAR CAM3 general circulation model (Flanner et al., 2007).

FTOA for tropospheric ozone as reported in Table 3 is the instantaneous forcing at the tropopause based on GISS model II' chemistry calculations for the 1880 to 2003 time period (Shindell et al., 2006). FTOA for methane is calculated at the tropopause from simulations for 1900 to 2001 driven by changes in all well-mixed greenhouse gases (WMGHGs) accounting for the fractional contribution of methane to the total forcing (0.20) and its efficacy relative to the total WMGHG efficacy (1.05/1.02). The role of methane in ozone production is included in the tropospheric ozone calculation.

3.2 Surface Temperature Response

Seasonally averaged values of the surface temperature response in the Arctic to forcings due to the short lived pollutants are shown in Table 3. The climate models used to calculate the Arctic response were forced globally with changing atmospheric composition. Values for tropospheric aerosol direct and indirect effects are based on GISS Model E climate simulations (Figure 11 of Hansen et al., 2007). Indirect effects only include the temperature response due to changes in cloud cover. Values are reported as the zonal mean temperature change for 1880 to 2003, where the 1880 simulation includes a small fossil fuel source and biomass burning emissions at half of present-day levels. Biofuel emissions are not included in these calculations. The temperature response due to deposition of BC on snow and ice surfaces was calculated with the SNICAR (Snow, Ice, and Aerosol Radiative model) coupled to the

NCAR CAM3 general circulation model using the same emissions scenario as described in the previous section (Flanner et al., 2007).

The temperature response due to forcing by tropospheric ozone and methane are based on GISS Model E calculations detailed in Shindell et al. (2006) and Hansen et al. (2007) using the regional averages and time periods described above. The surface temperature response resulting from increased cloud longwave emissivity is based directly on values of Fs reported in Table 3 (Garrett and Zhao, 2006).

3.3 Model Performance and Uncertainties

As these are the first Arctic estimates of seasonally averaged forcing for the short-lived pollutants as per Quinn et al. (2008), it is difficult to assess model performance by comparing to values calculated using other models. It is possible, however, to compare geographical distributions of aerosol species and forcing estimates averaged over annual and global scales. The NASA GISS model used in the calculation of the aerosol direct and indirect forcings was thoroughly compared to other global aerosol models as part of the AeroCom initiative. A comparison of black carbon mass in the polar regions that included sixteen models found that two models had greater than 7% of their BC mass in the Arctic, 5 had 6 to 7% of their BC in the Arctic, and nine had less than 6% of their BC in the Arctic (Textor et al., 2006). Falling within this range of variability, the GISS model had 7% of the BC in the Arctic. Hence, the GISS model was at the higher end of the range but was not an outlier.

Also as a part of the AeroCom initiative, Schulz et al. (2006) compared annually averaged total aerosol direct forcing from nine global aerosol models. The GISS model and one other (UIO_GCM) had the most positive values of aerosol direct forcing within the Arctic (0.02 to 0.05 W m^{-2} vs. 0.0 to 0.2 W m^{-2}) due to a larger load of BC transported to the region. However, a comparison of modeled BC concentrations from the GISS model to those measured at Spitsbergen and two Alaskan sites did not reveal systematic biases within the GISS model (Koch et al., 2007). The ratio of modeled to observed concentrations was found to be between 0.5 and 0.67 at Spitsbergen (i.e., model values were lower than observed) and between 0.67 to 1.5 at the two sites in Alaska.

Uncertainties in model calculations of the BC-snow forcing arise from emissions, effects of snow aging and meltwater scavenging, black carbon optical properties, and snow cover fraction with the contribution to uncertainty following the order listed. Based on uncertainties in these five factors, the potential range in black carbon-snow forcing is -87% to +240% relative to the central estimates given here. This large range is indicative of the current state of understanding of this forcing mechanism. On a global, annually averaged basis, the model used in this study produced a forcing estimate for fossil fuel and bio-fuel black carbon of +0.04 W m^{-2} which is slightly smaller than those reported by Hansen et al. (2005) (+0.05 W m^{-2}) and Jacobson (2004) (+0.06 W m^{-2}).

Global, annual average radiative forcing due to tropospheric ozone increases from the preindustrial to the present have been calculated in a number of models, though observational evidence to constrain these calculations is minimal. The time-evolving tropospheric ozone used in the GISS climate simulations discussed here was taken from Shindell et al. (2003). The adjusted global annual average radiative forcing due to preindustrial to present-day tropospheric ozone change in that study, 0.30–0.33 W m^{-2} depending on emissions, is near the center of the 0.25–0.45 W m^{-2} range (with a mean of 0.34 W m^{-2} and a standard deviation of 0.07 W m^{-2}) seen in the most recent IPCC assessment (IPCC, 2007). Additional uncertainties in the forcing due to tropospheric ozone come from lack of knowledge about preindustrial emissions of ozone precursors. Uncertainty in the global mean annual average radiative forcing due to methane increases from the preindustrial to the present is very small, at only 10% of the total forcing of 0.48 W m^{-2} (IPCC, 2007).

The sensitivity of the Arctic to either local or remote forcing has not been quantified across a number of models. Therefore, it is not possible to compare the responses reported here with other studies. It is possible to consider climate sensitivities, however, where the climate sensitivity is defined as the change in equilibrium global surface-air temperature due to a doubling of carbon dioxide. Climate sensitivity of the GISS and NCAR models used here are both 2.7°C which is in the middle of the range seen in current state-of-the-art global climate models (2 to 4.5°C) (Kiehl et al., 2006; Kiehl, 2007).

4. Seasonality and Magnitude of Forcing due to Short-Lived Pollutants and Surface Temperature Response

The significant impact of short-lived, warming non-CO_2 pollutants on temperature response globally and for the Arctic is shown in Figure 11. On a global, annually average basis, the temperature increase due to the sum of the short-lived warming pollutants is roughly 70% of that that due to CO_2. For the Arctic annual average, the response due to the sum of the short-lived warming pollutants is about 80% of that due to CO_2. The surface temperature response due to the BC – atmosphere forcing assumes that 1 W m^{-2} results in a 0.15° temperature change (IPCC, 2007). This assumption may underestimate the temperature response as it does not include enhancements in forcing due to the internal mixing of BC with other aerosol types (Ramanathan and Carmichael, 2008). In addition, the BC – atmosphere forcing is sensitive to the height of the BC-containing aerosol in the atmosphere. Forcing will be larger for BC above the surface because it can absorb the solar radiation reflected by low-lying clouds.

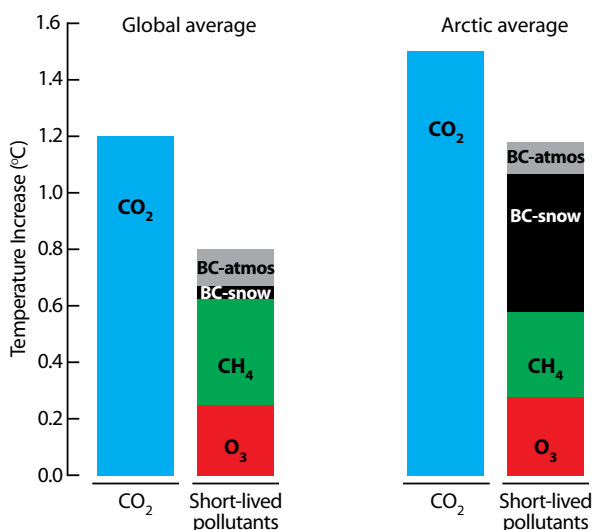As stated above, the magnitude of the forcing and temperature response due to each short-lived pollutant is a function of season. Hence, we now consider seasonally averaged values. Figure 12 provides a simplistic summary of the seasonal scenario of radiation, sources, and transport within the Arctic. Averaged over our defined Arctic region (60° to 90°N), forcing due to tropospheric ozone is at a maximum during spring (Table 3) when transport from lower latitude source regions is efficient, substantial ozone precursors persist from the winter buildup that occurs under conditions of low photochemical loss, and radiation is available for the photochemical production of ozone. Summertime forcing may also be significant, particularly when agricultural or boreal forest fire emissions increase ozone levels in the Arctic. The values shown in Table 3 for summertime are based on a standard climatology for present day biomass burning emissions (including forest fires) (Shindell et al., 2006). As such, they do not capture years with exceptionally large boreal fires.

Seasonal Scenario of Radiation, Sources, and Transport within the Arctic

Winter/Early Spring
● Solar radiation is limited so that the radiation balance is driven primarily by thermal fluxes
● Also the time of the year when transport of pollutants from the mid-latitudes is most efficient (Arctic Haze)
● Build-up of ozone and aerosol precursors

Spring
● Solar radiation becomes available for photochemical production of ozone and aerosols
● Transport of pollutants from mid-latitudes still efficient (Arctic Haze)
● Agricultural fires begin

Late Spring/Summer
● Solar radiation is at a maximum
● Surface melt begins
● Snow-albedo feedback maximizes
● More powerful greenhouse effect due to warmer temperatures
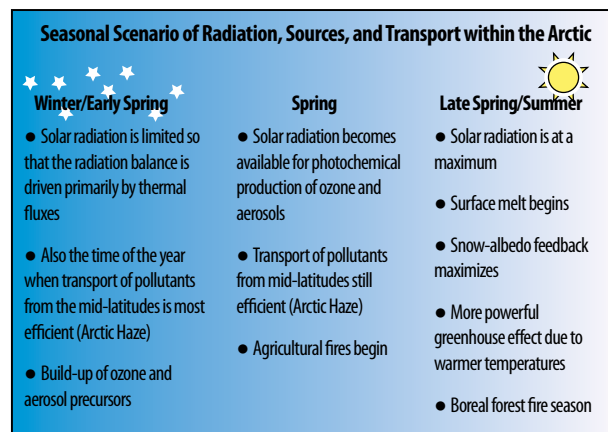● Boreal forest fire season

Figure 12. Seasonal scenario of radiation, sources, and transport within the Arctic.

Methane forcing, which is not limited by the seasonality of pollutant transport, is at a maximum during spring and summer due to warmer surface temperatures and, hence, a more powerful greenhouse effect. The surface response for both ozone and methane, indicated here as an increase in surface temperature of 0.43° and 0.34°C, respectively (Table 3 and Figure 13), is high in winter when the forcing is at a minimum. This offset implies that the Arctic surface temperature exhibits a delayed response to forcing (either local or extrapolar), is dynamically driven by forcings in other regions of the globe during this season, or is enhanced by erosion of the surface-based temperature inversion which is most prominent in winter.

In the Arctic, the magnitude and mechanism of climate forcing due to aerosols is controlled by an interplay among the seasonal timing of transport, available radiation, snow/ice melt, and deposition. In winter and early spring, when transport of pollutants from the mid-latitudes is most efficient, solar radiation is limited so that the radiation balance is driven

Figure 11. Annually averaged temperature increase for CO_2 and the short-lived warming pollutants relative to pre-industrial. Globally averaged values are shown on the left and Arctic averages on the right. Global values based on IPCC (2007). Arctic values based on Quinn et al. (2008). Note that cooling due to the short-lived pollutants is not included in this depiction. Such cooling may, although not necessarily, offset a portion of the warming (see discussion below).
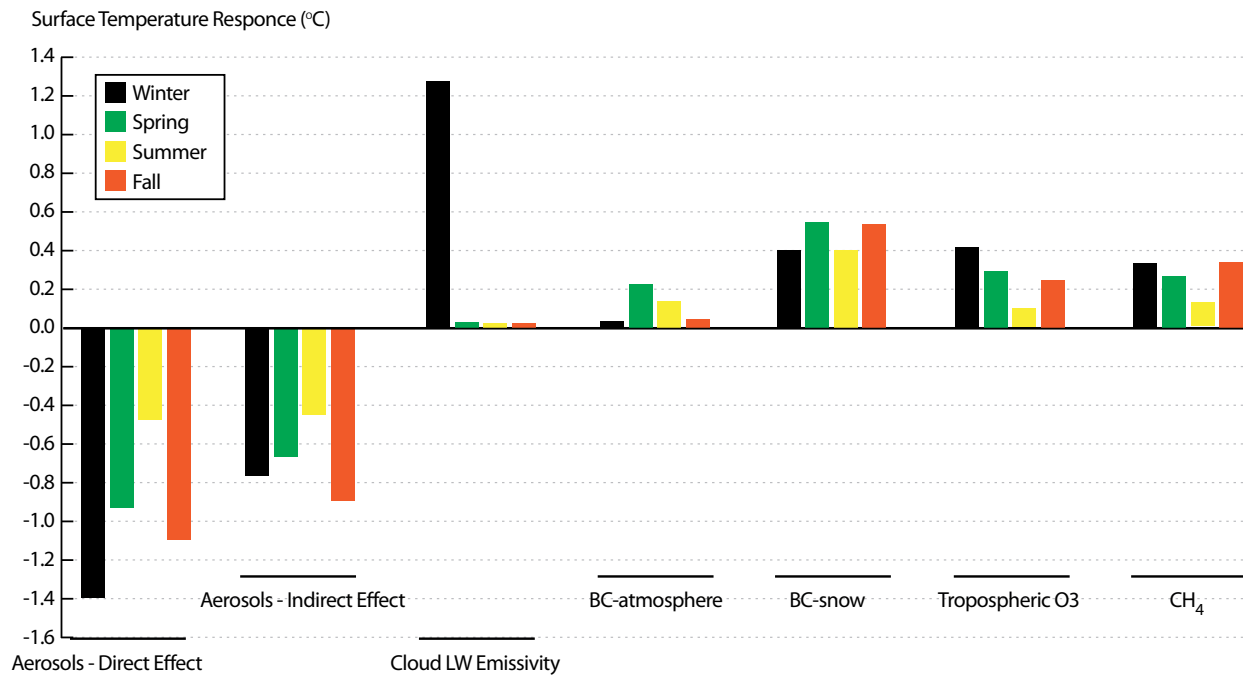
Surface Temperature Responce (°C)

Figure 13. Seasonally averaged values of temperature response at the surface for 60° to 90°N based on the calculations described in Section 3 and Table 3. Values for Cloud Longwave Emissivity are not seasonal averages as they only include times when pollution aerosol and clouds were coincident. Central values are plotted in cases where a range of values was reported in Table 3.

primarily by thermal fluxes. Interactions between the pollutant aerosol haze and the thin water clouds present at that time of year lead to an increase in longwave emissivity of thin clouds. Long-term ground based observations indicate that, when pollution and clouds are coincident, the result is a positive forcing at the surface of +3.3 to 5.2 W m^{-2} which is estimated to yield an enhanced surface warming of 1° to 1.6°C (Garrett and Zhao, 2006).

Concentrations of BC are elevated in the Arctic atmosphere during winter and spring due to the transport of Arctic Haze from the mid-latitudes. In the atmosphere, BC absorbs solar radiation which leads to a warming above and within the haze layer. This added heat increases the downward longwave radiation and warms the surface. This forcing is at a maximum in spring due to BC that has been transported from polluted source regions although it may also be significant in the summertime when boreal forest fire emissions reach the Arctic. The corresponding springtime surface temperature increase is about 0.24°C. The deposition of BC onto highly reflective snow/ice surfaces lowers the surface albedo and yields a positive surface forcing of 0.53 W m^{-2} in the spring, the season of maximum forcing (Flanner et al., 2007). The corresponding increase in surface temperature is about 0.56°C.

Finally, direct shortwave climate forcing by atmospheric aerosols occurs when solar radiation is abundant and springtime Arctic Haze or summertime fire plumes are present leading to a reduction in the amount of solar radiation reaching the surface. The result is a negative surface forcing during the spring (-0.72 W m^{-2} for the total fossil + bio-fuel + biomass burning aerosol) and a change in surface temperature of -0.93°C. As FS is an instantaneous forcing, this temperature change applies before the surface equilibrates with the warmer atmosphere. Additional effects include a reduction in Arctic sea level pressure and an increase in snow/ice cover. These aerosol impacts on circulation and the cryosphere may contribute to an offset, or phase lag, between the season of maximum forcing (spring and summer) and maximum temperature response (winter).

Mentioned in the discussion above but worth reiterating here is the offset between forcing and surface temperature response in several of the climate model simulations included in Table 3. Recently reported modeling results indicate that during the boreal summer, Arctic temperature response is well-correlated with either global or Arctic forcing (Shindell, 2007). During the non-summer seasons, however, the surface temperature response follows the global or Northern Hemisphere extratropical forcing more closely than local Arctic forcing, indicating that short-lived pollutants and their corresponding forcing in distant regions have a large impact on Arctic climate.

Conditions specific to the Arctic must also be considered when comparing the seasonality of forcing and the surface temperature response. For example, during the summer, the tropospheric aerosol indirect

effect has the largest value of FS but the smallest value of ∆TS. This discrepancy occurs because surface temperatures over the Arctic Ocean are limited as long as sea ice is present. This scenario (discrepancy between seasonal maxima in forcing and response) is likely to change with future decreases in sea ice extent.

The Arctic surface temperature response due to the short-lived warming pollutants is compared to that of the well-mixed greenhouse gases as a function of season in Figure 14. Despite the uncertainty in the model calculations described in Section 3, the potential contribution of the short-lived pollutants to observed accelerated warming in the Arctic is significant. Figure 13 shows the estimated cooling at the surface due to tropospheric aerosols. On a seasonally averaged basis, this cooling appears to offset the warming due to the short-lived pollutants. Certain sources, such as biomass burning, result in a haze layer that contains a high ratio of organic carbon to black carbon. In these cases, the net response due the atmospheric layer may be a net cooling. However, results of the direct effect forcing calculations shown in Table 3 suggest that organic carbon in a haze layer has a near neutral temperature response while black carbon has a positive temperature response. The temperature response due to indirect effects is less certain. In addition, on an episodic rather than seasonal basis the picture may be

quite different. For example, a short burst of heating due to absorption of radiation by BC on a snow/ice surface may lead to melting in the nonlinear climate system that is not offset by coincident cooling due to an aerosol layer above.
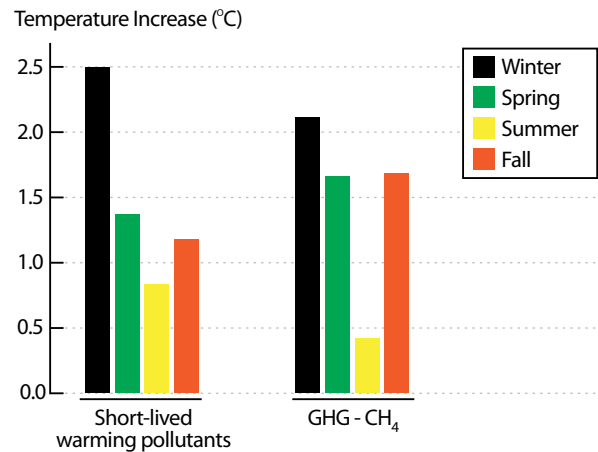

Figure 14. Seasonally averaged values of temperature response at the surface for 60° to 90°N for the short-lived pollutants that produce a warming at the surface (aerosols - cloud longwave emissivity forcing, BC - atmospheric and snow forcing, tropospheric O_3 – greenhouse gas and shortwave absorption forcing, methane - greenhouse gas forcing) and the well-mixed greenhouse gases excluding methane (GHG – CH_4).

5. Arctic Climate Mitigation Opportunities as Understood Today

Reducing emissions of CO_2 globally will reduce the rate of surface warming and snow/ice melt in the Arctic. However, targeting emissions of short-lived pollutants along with CO_2 has the advantage of impacting Arctic climate on a morenear-term timescale. The most effective mitigation strategy will target those pollutants that dominate surface radiative absorption. Specific mitigation opportunities include the following.

Methane. Reducing methane emissions will require targeting major controllable anthropogenic sources. Because of the relatively long lifetime of methane, reductions that benefit the Arctic can occur globally. The U.S. EPA has examined major methane sources and identified the following areas where considerable mitigation potential exists. These include worldwide coal mine desgasification and mine ventilation air capture, identification and repair of natural gas leaks, and better handling

of municipal solid wastes including using landfill methane as a source of energy. On a global basis, coal mine methane accounts for 8% of total methane emissions due to anthropogenic activities (U.S. EPA, 2006). Methane is removed from active mines with large ventilation systems and from both active and abandoned mines with degasification or gas drainage systems. Coal mine methane can be captured and used for power production, heating, and in manufacturing and industrial applications. Many of these CH_4 mitigation strategies are cost effective.

Ozone and black carbon – targeting source regions. Ozone and black carbon are not globally well mixed due to their relatively short lifetimes. Hence, specific source regions must be targeted to lessen their impacts in the Arctic. On timescales of days to weeks, northern Eurasia is the strongest source region for Arctic air pollution, especially in the lower troposphere (Barrie, 1986; Klonecki et al., 2003; Sharma et al., 2004; Stohl, 2006). Therefore, to decrease concentrations of ozone precursors and black carbon in the lower atmosphere, emissions in this region should be reduced. The source regions of short-lived pollutants in the upper Arctic atmosphere include

northern Eurasia and also areas in North America and Asia (Klonecki et al., 2003; Koch and Hansen, 2005; Stohl, 2006). Therefore, a substantial reduction of ozone and BC in the upper troposphere will require more widespread emission reductions throughout the northern hemisphere. The correspondence between surface temperature response in the Arctic and global and Northern Hemisphere extratropical forcings due to ozone emphasizes the need to reduce ozone on a northern hemisphere and global basis to reduce climate response in the Arctic. Finally, emissions of ozone precursors and BC within the Arctic should be kept at a minimum as these will have a disproportionately large impact on within-Arctic concentrations.

Ozone and black carbon – targeting sources. Reducing methane emissions as outlined above will decrease ozone production. Reductions in NO_x also will contribute but, at the same time, will decrease OH which is the major sink for methane. Hence, an ozone reduction strategy using NO_x controls that benefits climate will also include methane, NM-VOCs, and/or carbon monoxide reductions. Carbon monoxide forms when carbon in fuel does not burn completely. The main source of carbon monoxide is gasoline-powered vehicles. Abatement options include catalysts, routine inspection and maintenance, and addition of oxygen-containing compounds to gasoline (U.S. EPA, 1993). The majority of anthropogenic NMVOCs released into the atmosphere are from transportation sources and industrial processes utilizing solvents such as surface coating (paints), printing (inks), and petrochemical processing. The choice of NMVOC control measure is compound specific. Options include installation of control devices such as an incinerator, a solvent recovery system, limits on the amount of solvent used in products, and product stabilization (U.S. EPA, 1999). In addition to targeting transportation and industrial sources, reducing or eliminating agricultural fires in eastern Europe and northern Asia would effectively reduce CO, NMVOC, and ozone concentrations in the Arctic.

Reducing black carbon concentrations will require targeting sources that emit aerosols with a high absorptivity and relatively low reflectance (e.g., diesel combustion and residential stoves). Reducing within-Arctic emissions of black carbon (e.g., generators) and implementing emission controls on marine vessels operating within Arctic waters (particularly in light of the likely increase in shipping activity as the snow/ice pack decreases) will also be required. Additional strategies include reducing prescribed agricultural burns in eastern Europe so that black carbon emission and deposition does not occur in spring as radiation is increasing and the area of snow/ice pack is large. Reducing ozone and black carbon emissions has the added benefit of improving air quality and decreasing associated health hazards.

6. Future Directions for Research

Many of the impacts of short-lived pollutants on Arctic climate are not well understood or quantified. This lack of understanding is evident in the large range of potential forcing values calculated by single and multiple models as discussed in Section 3. This paper reports the results of Quinn et al. (2008) which were the first seasonally averaged forcing and temperature response estimates focused solely on the Arctic for a broad range of chemical species. As that was a first attempt, there is much work left to be done to more accurately quantify the impacts of each pollutant and to identify the most effective mitigation strategies. Specific scientific issues and areas of uncertainty in need of future research are discussed below.

Methane. Methane emissions from wetlands within the Arctic and sub-Arctic and from methane hydrate deposits in the Arctic resulting from rising surface temperatures are highly uncertain. Quantifying these emissions and how they might be expected to change in the coming years in response to rising temperatures is critical to understanding the impact of methane on Arctic climate as well as global climate.

Ozone. The effectiveness of controlling near-Arctic or within-Arctic NO_x emissions to reduce tropospheric ozone within the Arctic is unknown. Local NO_x emissions are likely to become significant if Arctic shipping activity increases as predicted. Research is needed to improve our understanding of reactive nitrogen chemistry and the oxidation capacity of the Arctic atmosphere. In addition, research is needed to determine how global ozone forcing impacts the Arctic.

Black carbon. Our understanding of deposition of black carbon-containing aerosol and trends in atmospheric concentrations of black carbon is constrained by limited measurements both in space and time. Questions concerning responsible source regions, transport, and atmospheric processing of

BC and other tropospheric aerosols persist in large part because of a paucity of historical and modern measurements of aerosol concentrations across the Arctic. Simultaneous pan-Arctic measurements of atmospheric and deposited BC combined with modeling studies are needed to identify sources, particularly those that impact the timing and rate of snow/ice melt, and to gain a better understanding of transport pathways and deposition processes. Recent measurements of BC and tracer species in Greenland ice cores demonstrated the power of this method for identifying source regions of BC at one site in the Arctic over the last 200 years (McConnell et al., 2007; McConnell and Edwards, 2008). Similar measurements at other Arctic sites where ice coring is possible are critical to identify differences in source regions of BC across the Arctic and how concentrations have changed as a result of historical and current emissions. This information can be used to assess the emission inventories used in global aerosol models and to evaluate model performance.

A comparison of 16 global aerosol models revealed that harmonizing aerosol sources has only a small impact on differences in calculated global aerosol burdens (Textor et al., 2007). Rather, the amount of BC estimated to be in the Arctic is dependent on model-specific treatment of vertical mixing, meridional transport, and aerosol removal (Textor et al., 2006; 2007). Measurements of atmospheric BC (or aerosol light absorption) are required across the Arctic and in the vertical to assess modeled transport and aerosol removal processes. Satellite observations of aerosol vertical and horizontal distributions also will help in model validation. High-time-resolution aerosol records from ice cores provide a means to evaluate model-simulated transport and removal processes as well as emissions inventories and to extend back in time modern atmospheric aerosol measurements (e.g., Sirois and Barrie, 1999).

Other tropospheric aerosols – surface warming. The enhancement of longwave emissivity from thin liquid-phase Arctic clouds due to interactions with anthropogenic aerosols may lead to significant surface temperature increases. These increases occur in phase with sea ice melt, potentially leading to a resonant amplification. As for black carbon, combined measurement and modeling studies are required to determine the source regions, chemical composition, and climate impact of different aerosol types. Measurements at sites with radiation instrumentation are particularly key so that information about aerosol and cloud properties, the impact of aerosols on cloud properties, and the

resulting impacts on the radiation budget can be assessed. In addition, further research is required to evaluate the role of aerosols in ice formation in low level mixed-phase clouds.

Other tropospheric aerosols – surface cooling. Reflective aerosols in atmospheric layers prevent incoming solar radiation from reaching the ground and yield a cooling at the surface. Hence, reductions in aerosol concentrations within the Arctic and in distant source regions may contribute to Arctic warming (Shindell, 2007). Assessing the overall impact of tropospheric aerosols in the Arctic (direct and indirect effects) is required to determine how reductions in aerosol concentrations will affect Arctic climate.

Feedbacks and Climate Responses. The feedback mechanisms that come into play due to the combination of forcings from all pollutants and the complexity of the Arctic environment are highly uncertain. Models are the only tool available to assess the climate response of individual and combined forcings and feedback mechanisms. In addition, models are required for predictions of climate impacts of the short-lived pollutants over the coming decades. The measurements described above will serve to constrain models thereby improving our predictive capability and our understanding of climate sensitivites to forcings. Modeling efforts required for a better understanding of feedbacks and climate responses include improved parameterizations of snow albedo and interactions between aerosol and mixed-phase clouds, studies that allow for the discrimination between forcings and feedbacks within the climate system, and multi-model comparisons aimed directly at emissions, transport, and atmospheric processes that impact the Arctic.

Mitigation. Modeling studies are required to determine the effectiveness of individual mitigation strategies on Arctic climate and, in particular, the surface temperature response. The choice of mitigation strategies is complicated as each pollutant source includes multiple chemical species (e.g., forest fires emit black carbon, organic carbon, and ozone). Accurate estimates of the climate impacts due to a specific mitigation strategy must take into account the simultaneous reduction of all species from a given source.

Scientific questions likely to be addressed by research within the next two years. At the November 2007 meeting on short-lived pollutants and their impact on Arctic climate (sponsored by NILU, IGAC, CATF, and CPC), the following list of research actions likely to be accomplished in the next two years was put forward:

- Identify source region-, sector-, and season-specific abatements for the optimal reductions in emissions of short-lived pollutants.

- Develop a better understanding of black carbon sources that result in deposition within the Arctic during winter and spring.

- Model the effects of individual mitigation strategies on Arctic climate.

- Identify the impact of short-lived pollutants on the Arctic cryosphere, particularly in regions where melting has been most dramatic (western Siberia).

- Determine and account for the post-deposition lifetime of black carbon on multi-year Arctic snow and ice and the impact on melting.

- Determine the global and Arctic-specific boreal forest fire climate impacts.

- Assess the role of short-lived pollutants in the early 20th century high latitude warming period.

- Assess Arctic climate impacts from the short-lived pollutant emissions associated with increased shipping activity and resource exploration within the Arctic.

- Assess the relative role of the short-lived pollutants and the associated impacts (including clouds) on the Arctic surface heat budget.

Additional required research activities:

- Support source identification by a fuller analysis of existing data and regional scale climate modeling (inverse and forward).

- Develop an Arctic monitoring network for short-lived aerosol pollutants which ensures appropriate spatial resolution and is tied to the needs of the modeling community for further model development and evaluation. This activity will require adding measurement capabilities to current sites, expanding the number of sites currently in operation, and ensuring full measurement capability at new sites. Required measurements include aerosol chemical composition to reveal information about anthropogenic and natural sources (e.g., sulfate, nitrate, organic carbon, black carbon, dust, and sea salt) and aerosol optical and radiative properties to assess climate impacts (e.g., light scattering and absorption and aerosol optical depth).

- The current network of sites (see: http://gaw.kishou.go.jp/wdcgg/) where CH_4 abundance and isotopic composition are measured should be expanded. A future network should be sufficiently dense to assess national inventories of natural and anthropogenic emissions, improve understanding of processes that emit CH_4, and better constrain inverse model studies of the methane budget. It should include measurements of multiple tracers, including CH_4 carbon and hydrogen isotopes. Continuous measurements of CH_4 abundance from tall towers and measurements of multiple species in vertical profiles of discrete samples are necessary components of the network. It is recommended that measurement programs quickly and easily make their data available to other scientists, and that governments simplify customs procedures for exchange of air samples among countries.

- The implementation of a mitigation strategy for BC reaching the Arctic requires a high confidence level in the monitoring of BC in the Arctic. To this end, it is necessary that the measurement techniques at each site are comparable. There are four sites in the Arctic conducting continuous measurements of BC: Barrow (Alaska, USA), Ny-Ålesund (Svalbard, Norway) Alert (Nunavut, Canada) and Summit (Greenland, Denmark), and several approaches to the measurement or estimation of BC are used. Some techniques are specific to BC, such as the thermal absorption analyses of samples of BC collected on filters, whereas some use a surrogate observation to define BC. A few make measurements of size segregated BC. Due to the variety of techniques, there is potential for relatively large uncertainty in the measurements of BC. Confidence that the changes in BC measured at each of the above Arctic sites accurately reflect changes Arctic-wide requires a strong and systematic intercomparison program. Such a program should follow the protocol of the WMO-GAW program for the measurement of BC, and the precision and accuracy of the BC reported at each site should be within limits defined by WMO-GAW (http://www.nilu.no/projects/ccc/manual/download/gaw153.pdf). An initial basis for the intercomparison can be the WMO-GAW Intercomparison of Nephelometers and Absorption Instruments held in Leipzig in March 2007. Beyond that a structure for intercomparisons needs to be developed and implemented by the coordinators of the BC measurements at each of the above four Arctic sites.

- Determine the inter-annual variability of synoptic transport patterns to the Arctic, in the context of past and predicted shifts in atmospheric transport patterns as a result of climate change, to add support to the development of mitigation strategies.

Some of these topic areas are covered, in part, by research that is being undertaken as part of the International Polar Year (IPY). Other research will require additional support.

References

Albrecht, B.A., Aerosols, cloud microphysics, and fractional cloudiness, Science, 245, 1227 – 1230, 1989.

Arctic Climate Impact Assessment (ACIA), Impacts of a warming Arctic, Cambridge University Press, Cambridge, UK, 2004.

Barrie, L. A.: Arctic air pollution—An overview of current knowledge, Atmos. Environ., 20, 643– 663, 1986.

Björk, R. G. and U. Molau, Ecology of alpine snowbeds and the impact of global change, Arctic, Antarctic and Alpine Research, 39, 34-43, 2007.

Bruhwiler, L.M. and E. Matthews, Can we reconcile our understanding of the atmospheric methane budget over the past decades with atmospheric observations? EOS Trans. AGU, 88, (52), Fall Meet. Suppl. Abstract B52C-03, 2007.

Cao, M., K. Gregson, and S. Marshall, Global methane emissions and its sensitivity to climate change, Atm. Env., 32, 3293 – 3299, 1998.

Chameides, W.L., F. Fehsenfeld, M.O. Rodgers, et al., Ozone precursor relationships in the ambient atmosphere, J. Geophys. Res., 97, 6037 – 6055, 1992.

Chapin, F.S., M. Sturm, M.C. Serreze, et al., Role of land-surface changes in Arctic summer warming, Science, 310, 657 – 660, 2005.

Christensen, T.R., T. Johansson, J. Akerman, et al., Thawing sub-arctic permafrost : Effects on vegetation and methane emissions, Geophys. Res. Lett., 31,doi:10.1029/2003GL018680, 2004.

Clarke, A.D. and K.J. Noone, Soot in the Arctic snowpack: a cause for perturbations in radiative transfer, Atmos. Environ., 19, 2045 – 2053, 1985.

Crutzen, P., A discussion of the chemistry of some minor constituents in the stratosphere and troposphere, Pure Appl. Geophys., 106-108, 1385-1399, 1973.

Dentener, F., D. Stevenson, J. Cofala, R. Mechler, M. Amann, P. Bergamaschi, F. Raes, and R. Derwent, The impact of air pollutant and methane emission controls on tropospheric ozone and radiative forcing: CTM calculations for the period 1990 – 2030, Atm. Chem. Phys., 5, 1731 – 1755, 2005.

Dlugokencky, E.J., S. Houweling, L. Bruhwiler, K.A. Masarie, P.M. Lang, J.B. Miller, and P.P. Tans, Atmospheric methane levels off: Temporary pause or new steady-state? Geophys. Res. Lett., 30, doi:10.1029/2003GL018126, 2003.

Fiore, A.M., D.J. Jacob, B.D. Field, D.G. Streets, S.D. Fernandes, and C. Jang, Linking ozone pollution and climate change: The case for controlling methane, Geophys. Res. Lett., 29(19),1919,doi:10.1029/2002GL015601, 2002.

Flanner, M.G., C.S. Zender, J.T. Randerson, and P.J. Rasch, Present-day climate forcing and response from black carbon in snow, J. Geophys. Res., 112, D11202, doi:10.1029/2006JD008003, 2007.

Fridlind, A.M., A.S. Ackerman, G. McFarquhar, G. Zhang, M.R. Poellot, P.J. DeMott, A.J. Prenni, and A.J. Heymsfield, 2007: Ice properties of single-layer stratocumulus during the Mixed-Phase Arctic Cloud Experiment (M-PACE): Part II, Model results. J. Geophys. Res., in press, 2007.

Garrett, T.J., C. Zhao, X. Dong, G.G. Mace, and P.V. Hobbs, Effects of varying aerosol regimes on low-level Arctic stratus, Geophys. Res. Lett., 31, doi:10.1029/2004GL019928, 2004.

Garrett, T.J. and C. Zhao, Increased Arctic cloud longwave emissivity associated with pollution from mid-latitudes, Nature, 440, 787 – 789, 2006.

Generoso, S., Bey, I., Attie, J.-L., and Breon, F.-M.: A satellite- and model-based assessment of the 2003 Russian fires: Impact on the Arctic region, J. Geophys. Res., 112, D15302, doi:10.1029/2006JD008344, 2007.

Girard, E., J.P. Blanchet, and Y. Dubois, Effects of Arctic sulfuric acid aerosols on wintertime low-level atmospheric ice crystals, humidity and temperature at Alert, Nunavut, Atm. Res., 73, 131 – 148, 2005.

Granier, C., U. Niemeier, J. H. Jungclaus, L. Emmons, P. G. Hess, J.-F. Lamarque, S. Walters, and G. P. Brasseur, Ozone pollution from future ship traffic in the Arctic northern passages, Geophys. Res. Lett., 33, L13807, doi:10.1029/2006GL026180, 2006.

Hagler, G. S. W., Bergin, M. H., Smith, E. A., Dibb, J. E., Anderson, C., and Steig, E. J: Particulate and water-soluble carbon measured in recent snow at Summit, Greenland, Geophys. Res. Lett.,. 34, L16505, doi:10.1029/2007GL030110, 2007.

Haagen-Smit, A.J., Chemistry and physiology of Los Angeles smog, Ind. Eng. Chem., 44, 1342-1346, 1952.

Hall, A. and X. Qu, Using the current seasonal cycle to constrain snow albedo feeback in future climate change, Geophys. Res. Lett., 33, L03502, doi:10.1029/2005GL025127, 2006.

Hansen, J. and L. Nazarenko, Soot climate forcing via snow and ice albedos, Proc. Natl. Acad. Sci., 101, 423 – 428, 2004.

Hansen, J., M. Sato, R. Ruedy, et al., Efficacy of climate forcings, J. Geophys. Res., 110, D18104, doi:10.1029/2005JD005776, 2005.

Hansen, J., Sato, M., Ruedy R., et al., Climate simulations for 1880 – 2003 with GISS modelE, Clim. Dyn., 10.1007/s00382-007-0255-8, 2007.

Harper, L.A., O.T. Denmead, J.R. Freney, and F.M. Byers, Direct measurements of methane emissions from grazing and feedlot cattle, J. Anim. Sci., 77, 1392 – 1401, 1999.

Houweling, S., T. Kaminski, F. Dentener, J. Lelieveld, and M. Heimann, Inverse modeling of methane sources and sinks using the adjoint of a global transport model, J. Geophys. Res., 104, 26137 – 26160, 1999.

Huang Y., R.L. Sass, and F.M. Fisher, A semi-empirical model of methane emission from flooded rice paddy soils, Glob. Change Biol., 4, 247 – 268, 1998.

IPCC (Intergovernmental Panel on Climate Change), 2001: Radiative forcing of climate change, in Climate Change 2001, Cambridge Univ. Press, New York, Cambridge University Press, 2001.

IPCC (Intergovernmental Panel on Climate Change), Summary for Policymakers, Contribution of Working Group I to the 4th Assessment Report, 2007.

Iversen, T. and E. Joranger, Arctic air pollution and large scale atmospheric flows, Atmos. Environ., 19, 2099 – 2108, 1995.

Jacobson, J.Z., Climate response of fossil fuel and biofuel soot, accounting for soot's feedback to snow and sea ice albedo and emissivity, J. Geophys. Res., 109, D21201, doi:10.1029/2004JD004945, 2004.

Johnson, D., K. Johnson, G.M. Ward, and M. Branine, Ruminants and other animals. In Kasischke, E.S., E.J. Hyer, P.C. Novelli, P. Bruhwiler, N. French, A.I. Sukhinen, J.H. Hewson, and B.J. Stocks, Influences of boreal fire emissions on Northern Hemisphere atmospheric carbon and carbon monoxide, Global Biogeochem. Chem. Cyc., 19, GB1012, doi:10.1029/2004GB002300, 2005.

Khalil, M.A.K., C.L. Butenhoff, and R.A. Rasmussen, Atmospheric methane: Trends and cycles of sources and sinks, Envron. Sci. Tech., 41, 2131 – 2137, 2007.

Kiehl, J.T., Twentieth century climate model response and climate sensitivity, Geophys. Res., Lett., 34, L22710, doi:10.1029/2007GL031383, 2007.

Kiehl, J.T., C.A. Shields, J.J. Hack, and W. Collins, The climate sensitivity of the Community Climate System Model: CCSM3, J. Climate, 19, 2854 – 2596, 2006.

Kirchgessner, D.A., S.D. Piccot, and J.D. Winkler, Estimate of global methane emissions from coal mines, Chemosphere, 26, 453 – 472, 1993.

Klonecki, A., P. Hess, L. Emmons, L. Smith, J. Orlando, and D. Blake: Seasonal changes in the transport of pollutants into the Arctic troposphere—Model study, J. Geophys. Res., 108(D4), 8367, doi:10.1029/2002JD002199, 2003.

Koch, D. and J. Hansen, Distant origins of Arctic black carbon: A Goddard Institute for Space Studies ModelE experiment, J. Geophys. Res., 110, D04204, doi:10.1029/2004JD005296, 2005.

Koch, D., T.C. Bond, D. Streets, N. Unger, and G.R. van der Werf, Global impacts of aerosols from particular source regions and sectors, J. Geophys. Res., 112, D02205, doi:10.1029/2005JD007024, 2007.

Korontzi, S., McCarty, J., Loboda, T., Kumar, S., and Justice, C.: Global distribution of agricultural fires in croplands from 3 years of Moderate Resolution Imaging Spectroradiometer (MODIS) data, Global Biogeochem. Cycles, 20, GB2021, doi:10.1029/2005GB002529, 2006.

Lubin, D. and A.M. Vogelmann, A climatologically significant aerosol longwave indirect effect in the Arctic, Nature, 439, 453 – 456, 2006.

Lubin, D. and A.M. Vogelmann, Expected magnitude of the aerosol shortwave indirect effect in springtime Arctic liquid water clouds, Geophys. Res. Lett., 34, doi:10.1029/2006GL028750, 2007.

MacCraken, M.C., R.D. Cess, and G.L. Potter, Climatic effects of anthropogenic Arctic aerosols: an illustration of climatic feedback mechanisms with one- and two-dimensional climate models, J. Geophys. Res., 91, 14445 – 14450, 1986.

McConnell, J.R., R. Edwards, G.L. Kok, et al., 20th century industrial black carbon emissions altered Arctic climate forcing, Science, 317, 1381 – 1384, 2007.

McConnell, J.R. and R. Edwards, Coal burning leaves toxic heavy metal legacy in the Arctic, Proc. Natl. Acad. Sci., in press, 2008.

Menon, S. and L. Rotstayn, The radiative influence of aerosol effects on liquid-phase cumulus and stratiform clouds based on sensitivity studies with two climate models, Clim. Dyn., 27, 345 – 356, 2006.

National Snow and Ice Data Center (NSIDC), Arctic sea ice shatters all previous record lows, NSIDC Arctic Sea Ice News Fall 2007, 1 October 2007.

Nakano, T., S. Kuniyoshi, and M. Fukuda, Temporal variation in methane emission from tundra wetlands in a permafrost area, northeaster Siberia, Atmos. Env., 34, 1205 – 1213, 2000.

Oltmans, S.J., I.E. Galbally, E.G. Brunke, et al., Trends of ozone in the troposphere, Geophys. Res. Lett, 25, 139 – 142, 1998.

Petit, J., J. Jouzel, D. Raynaud, et al., Climate and atmospheric history of the past 420,000 years from the Vostok ice core, Antarctica, Nature, 399, 429 – 436, 1999.

Prinn, R.G., R.F. Weiss, Miller, B.R. et al., Atmospheric trends and lifetime of CH3CCl3 and global OH concentrations, Science, 269, 187 – 189, 1995.

Pueschel, R.F. and S.A. Kinne, Physical and radiative properties of Arctic atmospheric aerosols, Sci. Tot. Env., 161, 811 – 824, 1995.

Quinn, P.K., G. Shaw, E. Andrews, E.G. Dutton, T. Ruoho-Airola, S.L. Gong, Arctic Haze: Current trends and knowledge gaps, Tellus, 59B, 99 – 114, 2007.

Quinn, P.K., T.S. Bates, E. Baum, N. Doubleday, A. Fiore, M. Flanner, A. Fridlind, T. Garrett, D. Koch, S. Menon, D. Shindell, A. Stohl, and S.G. Warren, Short-lived pollutants in the Arctic: Their climate impact and possible mitigation strategies, ACP, 8, 1723 – 1735, 2008.

Ramanathan, V. and G. Carmichael, Global and regional climate changes due to black carbon, Nature Geoscience, Advanced online publishing, 2008.

Ritter, C., J. Notholt, J. Fisher, and C. Rathke, Direct thermal radiative forcing of tropospheric aerosol in the Arctic measured by ground based infrared spectrometry, Geophys. Res. Lett., 32, doi:10.1029/2005GL024331, 2005.

Schulz, M., C. Textor, and S. Kinne et al., Radiative forcing by aerosols as derived from the AeroCom present-day and pre-industrial simulations, Atmos. Chem. Phys., 6, 5255 – 5264, 2006.

Seinfeld, J.H., Ozone air quality models: A critical review, J. Air Pollut. Control Assoc., 38, 616 – 645, 1988.

Serreze, M.C., M.M. Holland, J. Stroeve, Perspectives on the Arctic's shrinking sea-ice cover, Science, 315, 1533 – 1536, 2007.

Sharma, S., D. Lavoue, H. Cachier, L.A. Barrie, and S.L. Gong, Long term trends of the black carbon concentrations in the Canadian Arctic, J. Geophys. Res., 109, D15203, doi:10.1029/2003JD004331, 2004.

Sharma, S., E. Andrews, L.A. Barrie, J.A. Ogren, and D. Lavoue, Variations and sources of the equivalent black carbon in the High Arctic revealed by long term observations at Alert and Barrow: 1989 – 2003, J. Geophys. Res., 11, D14208, doi:10.1029/2005JF006581, 2006.

Shaw, G.E., Eddy diffusion transport of Arctic pollution from the mid-latitudes: a preliminary model, Atmos. Environ., 15, 1483 – 1490, 1981.

Shaw, G.E., The Arctic haze phenomenon, Bull. Am. Met. Soc., 76, 2403 – 2413, 1995.

Shaw, G.E. and K. Stamnes, Arctic haze: perturbation of the polar radiation budget, Am. N.Y. Acad. Sci., 338, 533 – 539, 1980.

Shindell, D., Local and remote contributions to Arctic warming, Geophys. Res. Lett., 34, L14704, doi:10.1029/2007GL030221, 2007.

Shindell, D. T., G. Faluvegi, and N. Bell, Preindustrial-to-present-day radiative forcing by tropospheric ozone from improved simulations with the GISS chemistry-climate GCM, Atm. Chem. Phys., 3, 1675-1702, 2003.

Shindell, D., G. Faluvegi, A. Lacis, J. Hansen, R. Ruedy, and E. Aguilar, Role of tropospheric ozone increases in 20th-century climate change, J. Geophys. Res., 111, D08302, doi:10.1029/2005JD006348, 2006.

Shindell, D., et al., A multi-model assessment of pollution transport to the Arctic, Atm. Chem. Phys. Disc., 8, 8385 – 8429, 2008.

Sirois, A. and L.A. Barrie, Arctic lower tropospheric aerosol trends and composition at Alert, Canada: 1980 – 1995, J. Geophys. Res., 104, 11599 – 11618, 1999.

Smol, J.P., A.P. Wolfe, H.J.B. Birks, et al., Climate-driven regime shifts in the biological communities of Arctic lakes, Proc. Nat. Acad. Sci., 102, 4397-4402, 2005.

Spahni, R., J. Chappellaz, T.F. Stocker, et al., Atmospheric methane and nitrous oxide of the late Pleistocene from Antarctic ice cores, Science, 310, 1317 – 1321, 2005.

Stohl, A.: Characteristics of atmospheric transport into the Arctic troposphere. J. Geophys. Res. 111, D11306, doi:10.1029/2005JD006888, 2006.

Stohl, A., E. Andrews, J. F. Burkhart, C. Forster, A. Herber, S. W. Hoch, D. Kowal, C. Lunder, T. Mefford, J. A. Ogren, S. Sharma, N. Spichtinger, K. Stebel, R. Stone, J. Ström, K. Tørseth, C. Wehrli, and K. E. Yttri, Pan-Arctic enhancements of light absorbing aerosol concentrations due to North American boreal forest fires during summer 2004, J. Geophys. Res. 111, D22214, doi:10.1029/2006JD007216, 2006.

Stohl, A., T. Berg, J.F. Burkhart, et al., Arctic smoke – record high air pollution levels in the European Arctic due to agricultural fires in Eastern Europe in spring 2006, Atmos. Chem. Phys., 7, 511 – 534, 2007.

Stroeve, J.C., T. Markus, W.N. Meier, J. Miller, Recent changes in the Arctic melt season, Ann. Glaciol., 44, 367 - 374, 2006.

Sundqvist, M.K, R.G. Björk, and U. Molau, Establishment of boreal forest species in alpine dwarf-shrub heath in subarctic Sweden, Plant Ecology and Diversity, 1, 67-75, 2008.

Textor, C., M. Schulz, S. Guibert, et al., The effect of harmonized emissions on aerosol properties in global models – an AeroCom experiment, Atmos. Chem. Phys., 7, 4489 – 4501, 2007.

Textor, C., M. Schulz, and S. Guibert et al., Analysis and quantification of the diversities of aerosol life cycles within AeroCom, Atmos. Chem. Phys., 6, 1777 – 1813, 2006.

Twomey, S., The influence of pollution on the shortwave albedo of clouds, J. Atmos. Sci., 34, 1149 – 1152, 1977.

US EPA, 1993. Automobiles and Carbon Monoxide, EPA 400-F-92-005.

US EPA, 1999. VOCs Controls, EPA/452/B-02-001

US EPA, 2006. Global Mitigation of Non- CO_2 Greenhouse Gases, EPA 430-R-06-005.

Walker, M. D. et al., Plant community responses to experimental warming across the tundra biome, PNAS, 103, 1342-1346, 2006.

Walter, K.M., S.A. Zimov, J.P. Chanton, D. Verbyla, and F.S. Chapin III, Methane bubbling from Siberian thaw lakes as a positive feedback to climate warming, Nature, 443, 71 – 75, 2006.

Warren, S.G. and W.J. Wiscombe, Dirty snow after nuclear war, Nature, 313, 467 – 470, 1985.

Wuebbles, D.J. and K. Hayhoe, Atmospheric methane and global change, Earth-Science Reviews, 57, 177 – 210, 2002.

Zimov, S. A., E.A.G. Schuur, and F. S. Chapin III, Climate change: Permafrost and the global carbon budget, Science, 312, 1612 – 1613, 2006.

Zwally, H.J., W. Abdalati, T. Herring, K. Larson, J. Saba, and K. Steffen, Surface melt-induced acceleration of Greenland ice-sheet flow, Science, 297, 218 - 222, 2002.